The structural development of the Orri dome, southern Variscan Pyrenes, Spain

PDF erstellt am: **17.05.2024**

The structural development of the Orri dome, southern Variscan Pyrenees, Spain

By Arie Speksnijder[1]

ABSTRACT

The Orri dome is a large anticlinal structure in the southern part of the Axial Zone of the Pyrenees. The Axial Zone consists of Paleozoic rocks that were deformed during the Variscan orogeny; some of these rocks have been metamorphosed during deformation, and late Variscan batholiths intruded in large volumes in the Pyrenees. Towards the south the Axial Zone is unconformably overlain by post-Variscan rocks (Westphalian D and younger), comprising Permian redbeds which were deposited in an elongated, east–west trending oblique-slip basin. These sediments are in turn unconformably covered by Triassic rocks, including Keuper evaporites, which served as a décollement horizon for the emplacement of an extensive nappe system during the Alpine orogeny in the Eocene. The nappe system mainly comprises Mesozoic and Tertiary rocks, but just south of the Orri dome allochthonous Variscan rocks crop out in the Nogueras Zone.

The Orri dome, entirely composed of a monotonous sequence of Cambro-Ordovician sediments in shallow marine facies, has been affected by a number of Variscan, post-Variscan, Alpine and post-Alpine deformation generations. Evidence for major Caledonian deformation is lacking.

In an early stage of the Variscan orogeny, open N–S and E–W folds were formed. These folds, developed on a 100's meters to kilometers scale, are not cut by an axial foliation. In contrast, the so-called mainphase deformation in the Axial Zone is characterised by tight, asymmetrical folds accompanied by a penetrative axial plane cleavage. Axial planes of macroscopic mainphase folds dip to the north and short foldlimbs are usually overturned. Mainphase structures are overprinted by a steep E–W fold system, occurring on all scales, that has strongly influenced older structures in the eastern part of the Orri dome. In a later stage of the Variscan orogeny relatively minor folds and kinkbands were formed.

Post-Variscan (pre-Mesozoic) deformation is basically of extensional nature, leading to cleavage fanning and the rare occurrence of kinkbands. Lateral movements took place as well, as all Variscan structures have been affected by dextral E–W shearing which mainly concentrated on pre-existing anisotropy planes. This shearing in the Variscan basement is considered to be of the same age, and caused by the same regional stress field, as superficial brittle faulting which controlled the sedimentation of Permian redbeds.

No traces of Mesozoic deformation can be detected in the Orri dome and direct surroundings. During the Alpine orogeny (Eocene–Oligocene), thrusting affected both the Axial Zone and its sedimentary cover. The impact of thrusting on the structure of the Orri dome is mainly expressed by the locally strong reorientation of Variscan cleavages. Like in the post-Variscan stage, post-Alpine faulting (and fracturing) is characterised by N–S extension and lateral movements, in this case probably of left-lateral sense.

The present-day outcrop of the Orri dome has been shaped by interference of the early and main Variscan deformations, later to be modified by post-Variscan and post-Alpine oblique-slip faulting and shearing, and thrusting of Alpine age.

[1]) Dept. of Structural Geology, State University Utrecht, Budapestlaan 4, Postbus 80021, 3508 TA, Utrecht, The Netherlands.

Present address: Koninklijke/Shell Exploratie en Produktie Laboratorium, Volmerlaan 6, 2288GD, Rijswijk (ZH), The Netherlands.

RÉSUMÉ

Le dôme Orri est une grande structure anticlinale de la partie sud de la Zone Axiale des Pyrénées. Celle-ci est composée de roches paléozoïques déformées durant l'orogénie varisque; certaines de ces roches ont été métamorphisées au cours des déformations, et ensuite les batholithes tardi-varisques, de grandes dimensions, se sont mis en place dans les Pyrénées. Vers le sud, la Zone Axiale est surmontée par des roches post-varisques (Westphalien D et plus jeune) en discordance, comprenant les grès rouges permiens, lesquels ont été déposé dans un bassin allongé de direction E–W, ayant fonctionné en décrochement. Ces sédiments sont à leurs tours recouverts en discordance par des roches d'âge triasique, incluant les évaporites du Keuper. Ces évaporites ont servi de niveau de décollement lors de la mise en place du système de nappes au cours de l'orogénie alpine à l'Eocène. Ce système de nappes comprend principalement des roches mésozoïques et tertiaires, mais, juste au sud du dôme Orri, des roches varisques allochtones affleurent dans la Zone Nogueras.

Le dôme Orri, entièrement composé de séquences monotones de sédiments cambro-ordovicien de faciès marin peu profond, a été affecté par de nombreux épisodes de déformations d'âge varisque, post-varisque, alpine et post-alpine. Cependant, il n'y a pas d'évidence de déformation d'âge calédonienne.

Au stade précoce de l'orogénie varisque, des plis ouverts de direction N–S et E–W se sont formés. Ces plis, d'échelle hectométrique à kilométrique, ne sont pas recoupés par une foliation axiale. En revanche, la «phase majeure» de déformation dans la Zone Axiale, est caracterisée par des plis serrés asymétriques accompagnés d'un clivage axial pénétratif. Les plans axiaux des plis macroscopiques de la phase majeure plongent vers le nord, et les flancs courts sont le plus souvent renversés. Aux structures de la phase majeure se superpose à toutes échelles un système de plis raides de direction E–W, qui a fortement influencé les structures plus anciennes dans la partie est du dôme Orri. A un stade tardif de l'orogénie varisque des plis relativement mineurs ainsi que des kinkbands se sont formés.

La déformation post-varisque (pre-Mésozoïque) est principalement de type extensive, ayant conduit à un basculement des clivages varisques et à l'apparition de rares kinkbands. De plus, des mouvements latéraux ont également pris place. Toutes les structures varisques ont été affectées par un cisaillement E–W dextre lequel a principalement réutilisé des plans d'anisotropie pré-existants. Ce cisaillement du socle varisque est supposé du même âge, et relié au même régime de contrainte régionale que les failles cassantes superficielles qui contrôlent la sédimentation des grès rouges permien.

Aucune trace de déformation mésozoïque n'a pu être détectée dans le dôme Orri et ses alentours. Au cours de l'orogénie alpine (Eocène–Oligocène), un système de chevauchements a affecté la Zone Axiale et sa couverture sédimentaire. Localement, l'impact de cette compression sur la structure du dôme Orri est exprimé essentiellement par une forte réorientation des clivages varisques. Comme pour l'étage post-varisque, la fracturation post-alpine est caractérisée par une extension N–S et des mouvements latéraux; dans ce cas probablement de type sénestre.

La forme actuelle du dôme Orri a été structurée par l'interférence des déformations varisques précoce et majeure, modifiée plus tard par les cisaillements et décrochements post-varisques et post-alpin, ainsi que par la compression d'âge alpine.

Introduction

Within the Alpine mountain belt of the Pyrenees a large mass of Variscan rocks is exposed, which is commonly referred to as the Axial Zone (Fig. 1). The Axial Zone consists of deformed sedimentary, metamorphic and intrusive rocks of pre-Stephanian age (ZWART 1979), intruded by undeformed late Variscan batholiths, and unconformably overlain by post-Variscan rocks. The large-scale Variscan structure of the Axial Zone comprises a number of E–W trending anticlines and synclines, like the Orri "dome" (SCHMIDT 1931; HARTEVELT 1970) in the south-central part of the Variscan outcrop. This complicated structure can be traced some 45 km along strike (Fig. 1 and 2), and has an exposed width of about 12 km. Its true width is not known, as the southern flank of the Orri dome is unconformably covered by Stephanian, Permian and Lower Triassic rocks. Towards the north, the Orri dome is bordered by the narrow Llavorsi syncline (Fig. 2).

The Orri dome is almost entirely built of very thick, unfossiliferous, non-metamorphic to very low-grade Cambro-Ordovician sediments of the *Seo Formation* (HARTEVELT
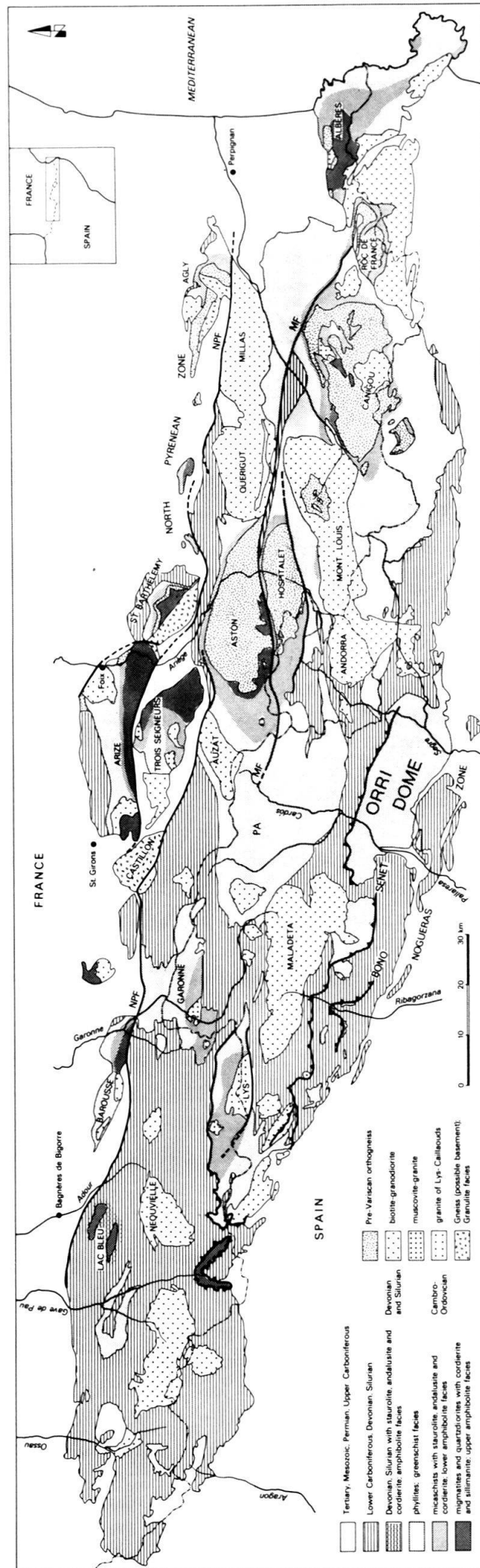
Fig. 1. Geological map of the outcrop area of the Variscan Pyrenees (the Axial Zone). The Orri dome is situated in the south-central part of the Axial Zone.

Legend:

- Tertiary, Mesozoic, Permian, Upper Carboniferous
- Lower Carboniferous, Devonian, Silurian
- Devonian, Silurian with staurolite, andalusite and cordierite, amphibolite facies
- phyllites, greenschist facies
- micaschists with staurolite, andalusite and cordierite, lower amphibolite facies
- migmatites and quartzdiorites with cordierite and sillimanite, upper amphibolite facies

- Pre-Variscan orthogneiss
- biotite-granodiorite
- muscovite-granite
- granite of Lys- Caillaouds
- Gneiss (possible basement), Granulite facies

Devonian and Silurian

Cambro-Ordovician

FRANCE

SPAIN

MEDITERRANEAN

NORTH PYRENEAN ZONE

ST BARTHELEMY
ARIZE
TROIS SEIGNEURS
CASTILLON
FOIX
AUZAT
ASTON
HOSPITALET
ANDORRA
MONT LOUIS
CANIGOU
QUERIGUT
MILLAS
AGLY
ALBERES
ROC DE FRANCE
ORRI DOME
SENET
BONO
NOGUERAS ZONE
MALADETA
GARONNE
BAROUSSE
NEOUVIELLE
LAC BLEU
LYS
PA

Perpignan
St Girons
Bagnères de Bigorre

NPF
NMF
PMF

Ariège
Cardós
Adour
Garonne
Gave de Pau
Ribagorzana
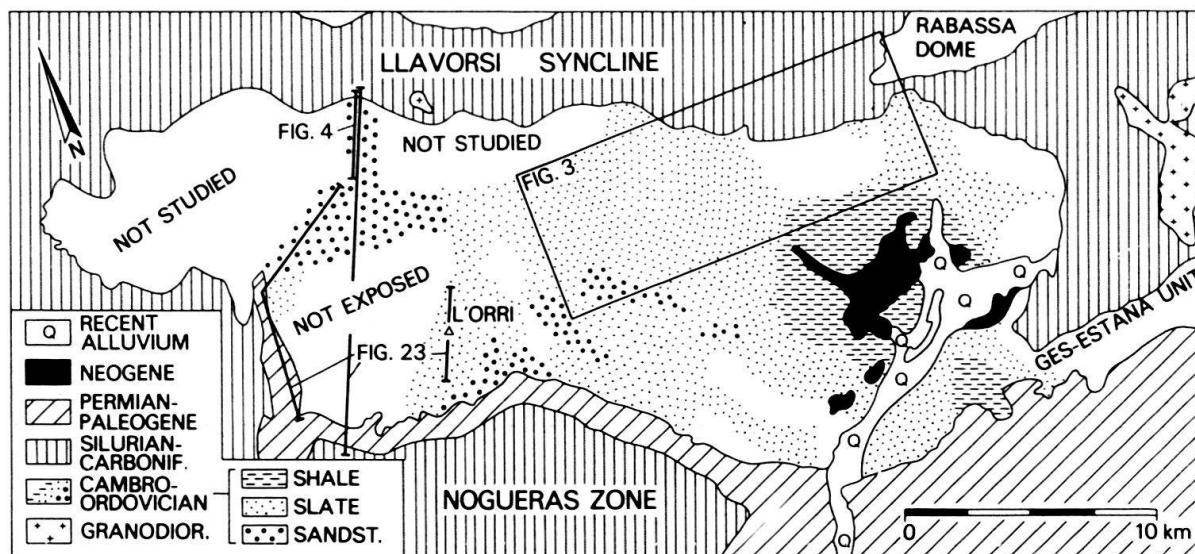Aragón
Ossau

0   10   20   30 km

Fig. 2. Simplified geological map of the Orri dome and surroundings. The following lithologies are indicated in the Cambro-Ordovician Seo Formation: sandstone (and quartzite, Fig. 5 b), slate (usually a regular monotonous interlayering of clay and sand on cm scale, Fig. 5 a), and shales (silt- and clay size, often a "pencil-shale" in case of strong cleavage development). The profile lines of Figures 4 and 23 and the map area of Figure 3 are shown. Upper Ordovician rocks crop out in the northeastern part of the dome and in the Ges-Estana unit (HARTEVELT 1969).
Note: this is not a palinspastically restored map; it shows the present (deformed) lithotype distribution.

1970), probably deposited in a shallow marine environment. They are characterised by a monotonous alternation of thin slates, silts and sand layers (up to a few centimeters thickness), although locally shales and silts may be much thicker. In some cases, individual sandstone and quartzite layers reach thicknesses of some meters to some tens of meters. Marker horizons are completely lacking within the Cambro-Ordovician rocks. The present distribution of lithotypes in the Seo Formation of the Orri dome seems to be determined by variations in sedimentary facies, rather than by structural organisation (Fig. 2).

On the northern flank of the Orri structure, at the transition to the Llavorsi syncline, some higher stratigraphic units crop out (from bottom to top, data mainly after HARTEVELT 1970):

The *Rabassa Conglomerate Formation* of Caradoc age, which in spite of its very coarse-grained nature overlies the Cambro-Ordovician here conformably; the *Cava Formation,* mainly built of sandstones, which may be up to 850 m thick east of the Orri dome but gradually wedges out along its northwestern border; the *Estana Formation* is a marl and limestone unit; the *Ansobell Formation,* developed over the whole Pyrenees, consists of black shales which replace the sandstones of the Cava Formation towards the north; the *Bar Quartzite* is a thin sandsheet, which only occurs in the south-central part of the Axial Zone; and finally the black carbonaceous shales of the *Silurian.* In the synclinal units of the Axial Zone, the Silurian is conformably overlain by predominantly calcareous and marly rocks of Devonian and Early Carboniferous age.

The conformable superposition of sediments from Cambro-Ordovician to Carboniferous age, without any significant hiatus, excludes the occurrence of major Caledonian deformation in the Pyrenees. The main phase of Variscan deformation took place in the Westphalian (ZWART 1979). In the post-orogenic stage, Stephanian slope breccias, tuffs,

andesitic basalts and alluvial sediments were deposited in fault-bounded sedimentary basins (Aguiro, Erill Castell and Malpas Formations of MEY et al. 1968). During the Permian, elongated strike-slip basins developed locally, which were rapidly filled with often coarse-grained redbeds (SPEKSNIJDER 1985; NAGTEGAAL 1969). The importance of post-Variscan strike-slip movements to the Orri dome will be one of the main subjects of this article.

Finally, after a period of erosion, a Lower Triassic conglomerate (part of the Bunt-sandstein) was laid down unconformably on one of the previously mentioned post-Variscan formations, or directly on the Variscan basement, as is the case along part of the southern boundary of the Orri dome. The Buntsandstein and its younger cover suffered from Alpine deformation, which left its mark in the essentially Variscan Orri dome as well. The marls of the Keuper, which overlie the Buntsandstein, acted as a décollement horizon for an extensive thrust system of Alpine (Eocene) age, which includes Variscan rocks in the so-called Nogueras Zone (SEGURET 1970), directly south of the Orri dome (Fig. 1 and 2).

East and south of the dome, rocks of Tertiary (up to Miocene) age are offset by faults on different scales, indicating post-Alpine brittle deformation which influenced the Orri dome as well.

Structural interpretation in the Orri dome is seriously hampered by the lack of marker horizons in the Cambro-Ordovician rocks of the Seo Formation. Hence, emphasis had to be laid on the analysis of directional data of the various structural elements; in total over 20 000 measurements were collected on the orientations of planar surfaces and lineations. In the following chapters the characteristics of successive deformation generations in the Orri dome will be discussed in detail. Distinction is made, in chronological order, between deformation of Variscan, post-Variscan, Alpine and post-Alpine age.

Variscan deformation

Pre-mainphase deformation (D_{V1} & D_{V2})

The most important Variscan deformational event in the Pyrenees, the mainphase folding, has for a long time been considered the oldest in the Variscan orogenic evolution. The occurrence of still older folds which are transected by the mainphase cleavage, was nevertheless recognised by various authors in the sixties (e.g. BOSCHMA 1963; MEY 1967b, 1968). Pre-mainphase folds, also called pre-cleavage folds, can in many cases easily be detected if marker horizons are available to show interference patterns between main-phase folds and earlier structures. Such a technique, however, cannot be applied to the monotonous slates and sandstones of the Orri dome. For this reason, a directional analysis of mainphase structural elements was carried out by SPEKSNIJDER (1987), who shows that two generations of pre-mainphase folding must have occurred in the northern part of the dome (Fig. 3).

In both cases the folds appear to be very open (interlimb angles at least 115°) and to have subvertical axial planes and subhorizontal foldaxes. There is, on the other hand, an important difference in strike direction of the axial planes: approximately north-south for the oldest generation of pre-mainphase folds, and approximately east-west for the younger. The folds of both systems appear to be symmetrical in profile.
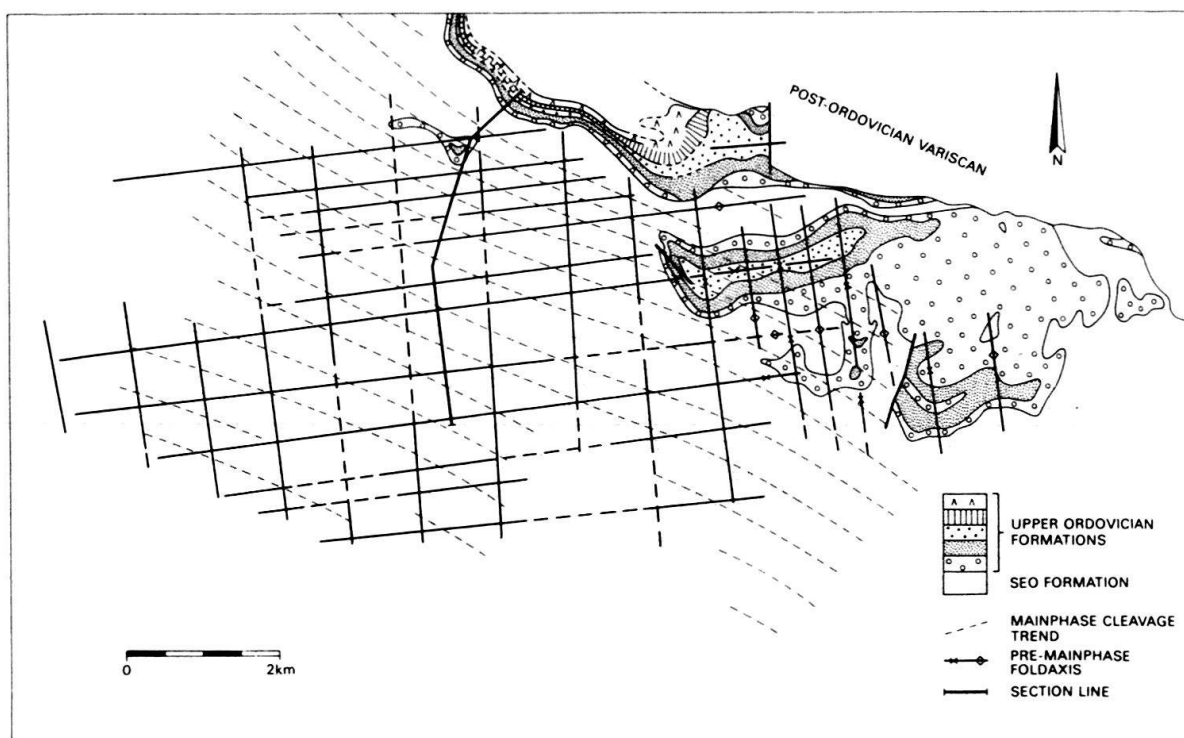
Fig. 3. Pre-mainphase structures in the northern part of the Orri dome; location shown in Figure 2. This schematic structural map shows N–S trending (D_{V1}) and E–W trending (D_{V2}) pre-mainphase foldaxes. Mainphase cleavage trend is WNW–ESE. The locations of pre-mainphase foldaxes within the Seo Formation are defined by sudden changes in orientation of intersection lineations of sedimentary bedding and mainphase cleavage. It is usually impossible to distinguish between synformal and antiformal axes when applying this technique. The section indicated on this map is shown in SPEKSNIJDER (1987); for related stereographic projections see Figure 6.

The structural significance of the occurrence of pre-mainphase folds in the Pyrenean Variscan evolution is discussed by SPEKSNIJDER (1987). They have been generated at the transition from a divergent to a convergent oblique-slip setting of the Variscan mobile belt (D_{V1}), and to an early stage of deformation resulting from continent–continent collision (D_{V2}).

Mainphase deformation (D_{V3})

Mainphase structures can be traced all over the Variscan Pyrenees (which does not necessarily imply they are everywhere of the same age), and mainphase cleavage is the major foliation in the Axial Zone. Mainphase folds in the Orri dome can be studied best in its northern part, where the effects of later Variscan and Alpine overprinting are negligible. The mainphase deformation (F_1 of ZWART 1979; F_2 of HARTEVELT 1970) is characterised by south-vergent asymmetrical folds, developed on all scales between some millimeters and one or more kilometers (Fig. 4 and 5a). Generally, long fold limbs exhibit shallow dips towards the north (Fig. 4a,b; 5b; 6a), whereas short limbs are usually overturned, thus dipping (steeply) north as well (Fig. 4a,b; 5c; 6a). Very often a penetrative axial plane cleavage is associated with mainphase folds (Fig. 4a,c; 5b,c; 6b), which may show convergent fanning in the fold profile. Generally the cleavage is a slaty cleavage in fine-grained sediments (Fig. 5c), or a spaced cleavage in sandstones (Fig. 5b). In some cases a crenulation cleavage does occur, folding sedimentary lamination on a
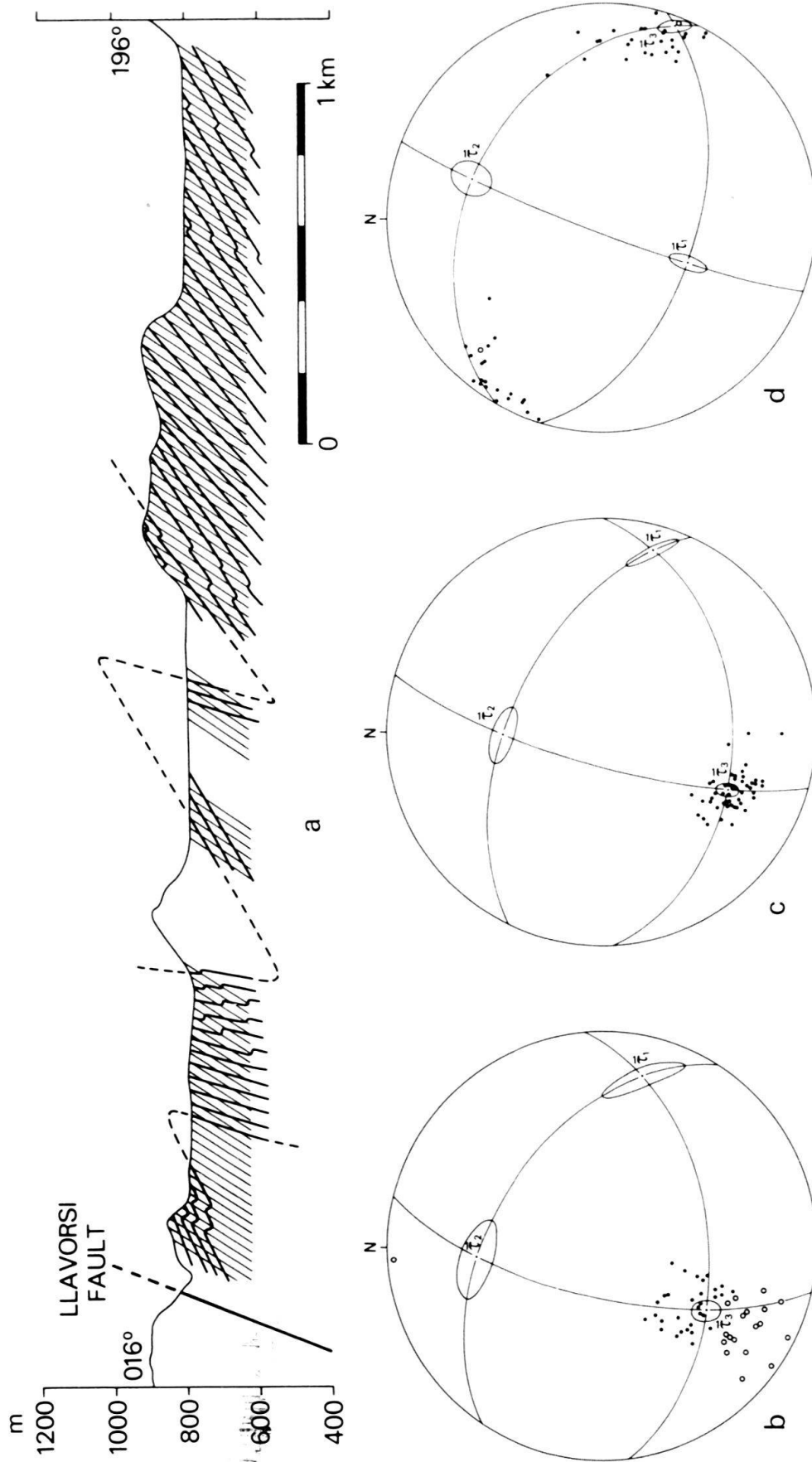
Fig. 4. Representative structural profile and associated stereographic projections of mainphase folds.

a) North–south structural profile along the Rio Noguera Pallaresa showing the orientations of mainphase cleavage (thin lines) and sedimentary bedding (thick lines) within Cambro-Ordovician rocks. Devonian sediments crop out north of the Llavorsi fault. The position of this profile is indicated on Figure 2 and 7.

b) Equal area projection of poles to sedimentary bedding. Discrimination is made between data from long foldlimbs (dots) and short limbs (open circles); confidence ellipses (at 95% confidence level) are drawn around these eigenvectors (see SPEKSNIJDER 1987). Number of measurements: N = 50.

c) Poles to mainphase cleavage. Note the strong coplanarity of the cleavage planes as indicated by the small size of the $\bar{\tau}_3$ confidence ellipse (95% confidence level). Number of measurements: N = 52.

d) Intersection lineations of sedimentary bedding and mainphase cleavage (dots), and small-scale mainphase foldaxes (open circles). Number of measurements: N = 48. Confidence ellipse at 95% confidence level.

5a

5b

5c

Fig. 5. Photographs of D_{V3} structures. For locations see Figure 7.
a) Small-scale mainphase fold in the southwestern part of the Orri dome. Penetrative axial plane cleavage has not developed in this case. The axial plane of the fold is only gently dipping north (towards the right).
b) Spaced mainphase cleavage in flat-lying sandstones on the long limb of a macroscopic mainphase fold. Located in the central-northern part of the dome where no significant overprinting of mainphase structures does occur. North towards the left.
c) Steep overturned bedding (parallel to the hammer shaft), and relatively steeply north dipping slaty cleavage, developed in very fine-grained sediments in the northern part of the dome. North towards the right.

micro-scale. In areas of large strain, e.g. on the inner arcs of fold hinges, differential layering has sometimes developed parallel to the mainphase foliation. Intersection lineations between sedimentary bedding and mainphase cleavage are well developed throughout the Orri dome (Fig. 4d; 6c), although on some long flanks of mainphase folds, especially in sandstones, cleavage and intersection lineations may be absent.

Mainphase structures are non-cylindrical and show an unusually large spreading of intersection lineation directions in the cleavage plane (Fig. 6c), which is attributed to the
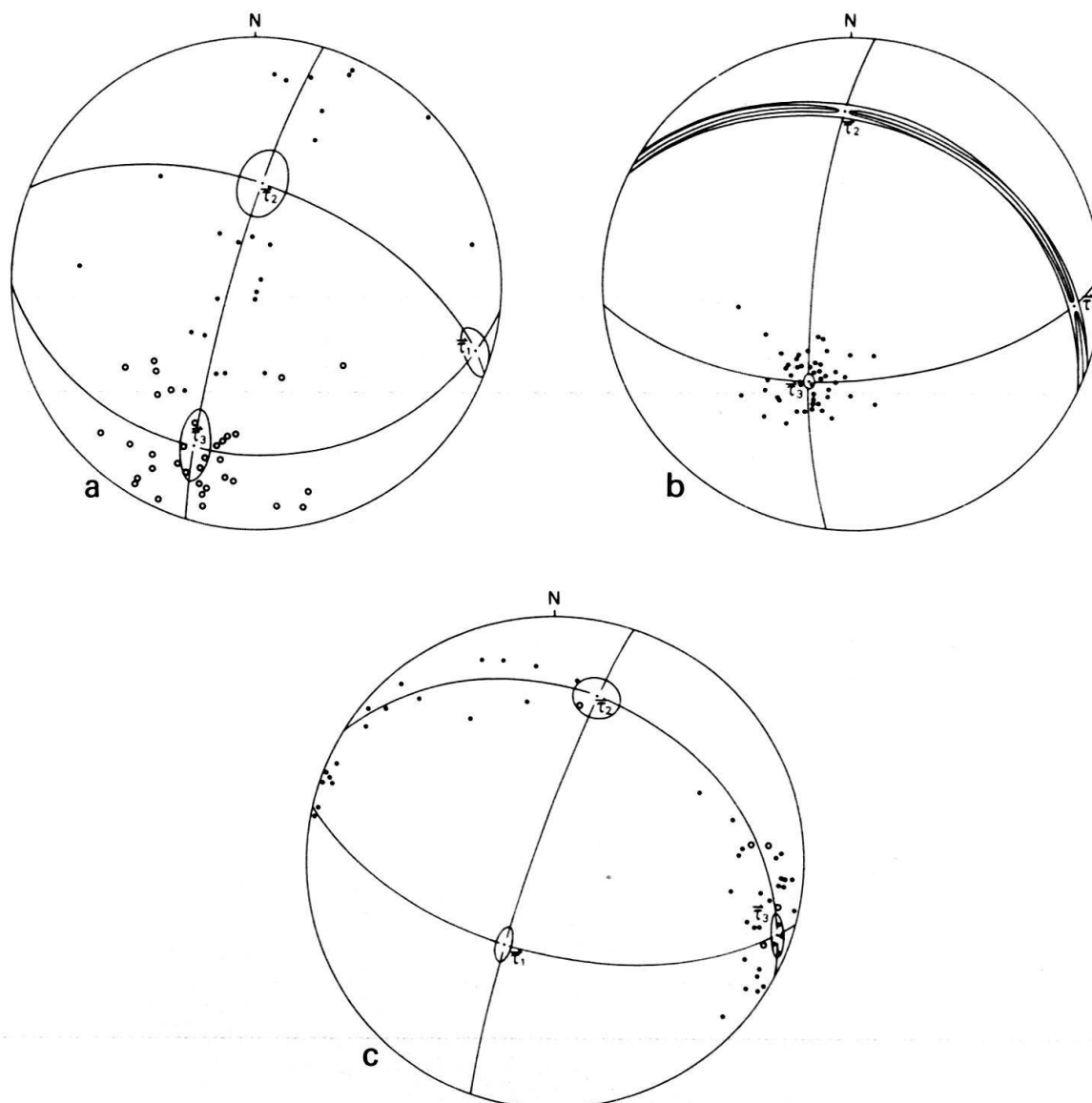
Fig. 6. Equal area stereographic projections of structural elements from the profile indicated in Fig. 3. In all three cases the eigenvector directions and their confidence ellipses for the orientation tensors of the distributions are indicated (from SPEKSNIJDER 1987). All confidence ellipses at 95 % confidence level.
a) Poles to sedimentary bedding. Dots indicate normal polarity of the beds, open circles represent reverse polarity (on overturned short foldlimbs). Number of measurements: N = 57.
b) Poles to mainphase cleavage. N = 51.
c) Intersection lineations of sedimentary bedding and mainphase cleavage (dots), and small-scale mainphase foldaxes (open circles). N = 54.

occurrence of pre-mainphase folds (SPEKSNIJDER 1987). Large-scale mainphase fold axes are subhorizontal and are directed WNW–ESE.

In the northwestern part of the Orri dome, the orientation of the mainphase cleavage is very constant (Fig. 4 and 7), which indicates that the cleavage has not been affected by major later deformation. In the rest of the dome, however, strong reorientation of the mainphase cleavage has taken place. In the western and southwestern part, the main-phase cleavage dip-angle gradually decreases towards the south, until it eventually occu-
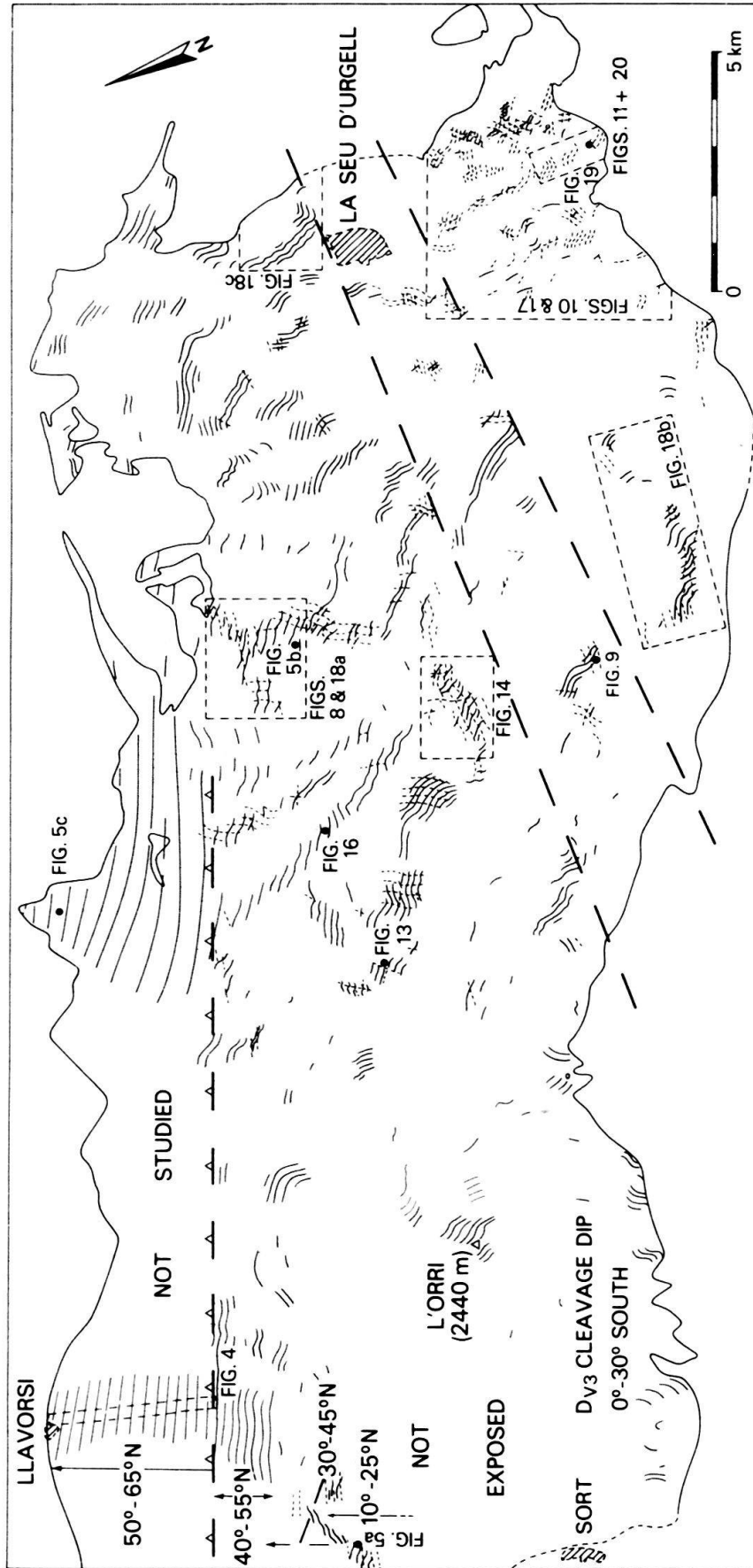
Fig. 7. Cleavage trend map of the Orri dome; the outline of the structure is defined by the outcrop area of the Seo Formation. This map is based on almost 3000 cleavage measurements. Shown are traces of mainphase cleavage (continuous lines), traces of D_{V4} cleavage (dashed, E–W trending), and traces of D_{V5} cleavage (dashed, N–S trending). Heavy dashed lines indicate the positions of postulated faults: an Alpine thrust in the north and post-Alpine faults in the south (for discussion see text). Numbers in the western part of the dome refer to mainphase cleavage dips. Boxes outline areas covered by other figures; dots show positions of photographs.

pies a subhorizontal position. The cleavage then abruptly changes dip direction and may dip as much as 30° to 35° towards the south along the southwestern rim of the Orri structure (Fig. 7). This change in orientation is not an original feature of the mainphase cleavage development: it will be shown later that Alpine thrusting is responsible for most of the rotation of Variscan structures and cleavages.

In the central, southern and eastern parts of the Orri structure, the cleavage has been gently to strongly folded during later Variscan deformation, as will be discussed in the following sections.
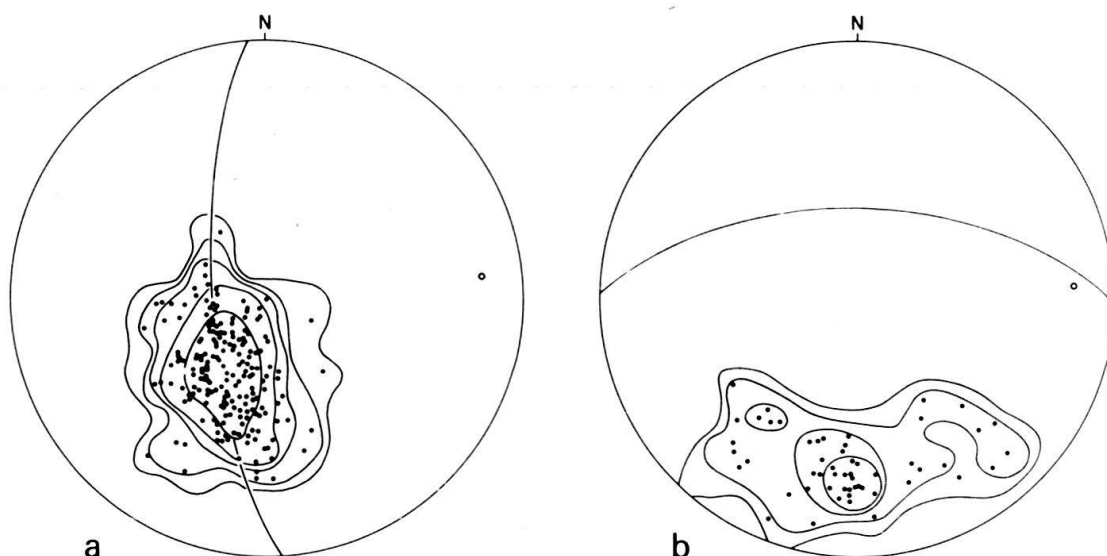

Fig. 8. The impact of D_{V4} deformation on the orientations of older structures in the central Orri dome. For location see Fig. 7.

a) Poles to folded D_{V3} cleavage; equal area projection. The open circle indicates the (apparent) foldaxis, see Fig. 18a. Number of measurements: N = 195. Contours: 1, 2, 5, 10, and 25 poles per 1 % area (0.5, 1.0, 2.6, 5.1, and 12.8% per 1 % area).

b) Poles to D_{V4} cleavage. This projection shows that this cleavage has been slightly folded (by D_{V5} and D_{PV1} deformation), but as the spreading is only limited, the maximum of the distribution is taken to represent the average D_{V4} pole, thus ignoring later deformation. The great circle represents the corresponding averaged D_{V4} orientation. The foldaxis of the D_{V3} cleavage (open circle, Fig. 8a) lies approximately within the (averaged) D_{V4} cleavage plane, which it should since D_{V4} is an axial plane cleavage. Number of measurements: N = 57. Contours represent 1, 2, 5, and 10 poles per 1 % area (1.7, 3.5, 8.1, and 17.5% per 1 % area).

First Variscan refolding (D_{V4})

In the central part of the Orri dome, mainphase structures are often overprinted by tight macroscopic folds (dm to m scale), that do not seem to affect the enveloping surface of the earlier folds significantly. The folds of the first Variscan refolding generation in this area (corresponding to the F_4 phase of HARTEVELT 1970, and ZWART 1979) have subvertical axial planes and gently plunging foldaxes (Fig. 8). Axial planes strike approximately E–W and the D_{V4} folds are asymmetric showing a Z-shape when looking east (Fig. 9).

Inspection of the cleavage-trend map of the Orri dome (Fig. 7) and stereographic projections (Fig. 8) shows that the influence of D_{V4} folding on mainphase structures is much more widespread and occurs on a larger scale than outcrop study does suggest. In plan view, the mainphase cleavage can be traced across km scale, seemingly very open

Fig. 9. D_{V4} folds in the southern part of the Orri dome (Fig. 7). The hammer rests on – and its shaft is parallel to – a long D_{V4} fold limb. The overall asymmetry of the folds is Z-shaped. View towards the east.
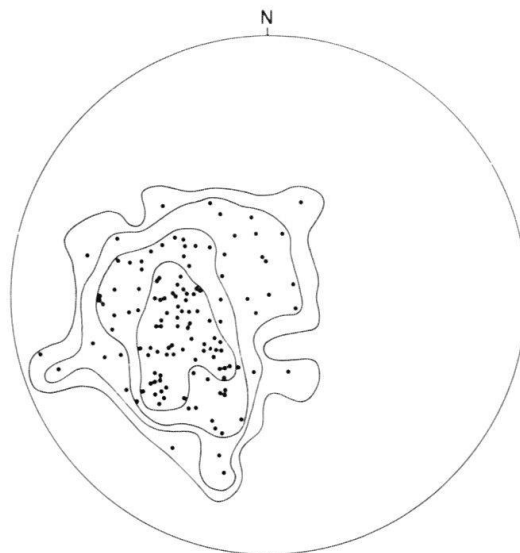

Fig. 10. Stereographic projection of poles to D_{V3} cleavage in the south-eastern Orri dome (Fig. 7), showing the accumulated effects of post-mainphase deformation. The spreading in N–S direction must be mainly attributed to D_{V4} folding. The orientation of D_{V4} cleavages in the same area is shown in Fig. 17. Number of measurements: N = 129; contours represent 1, 2, 5, and 10 poles per 1 % area (0.8, 1.6, 3.9, and 7.8 % per 1 % area).

11a
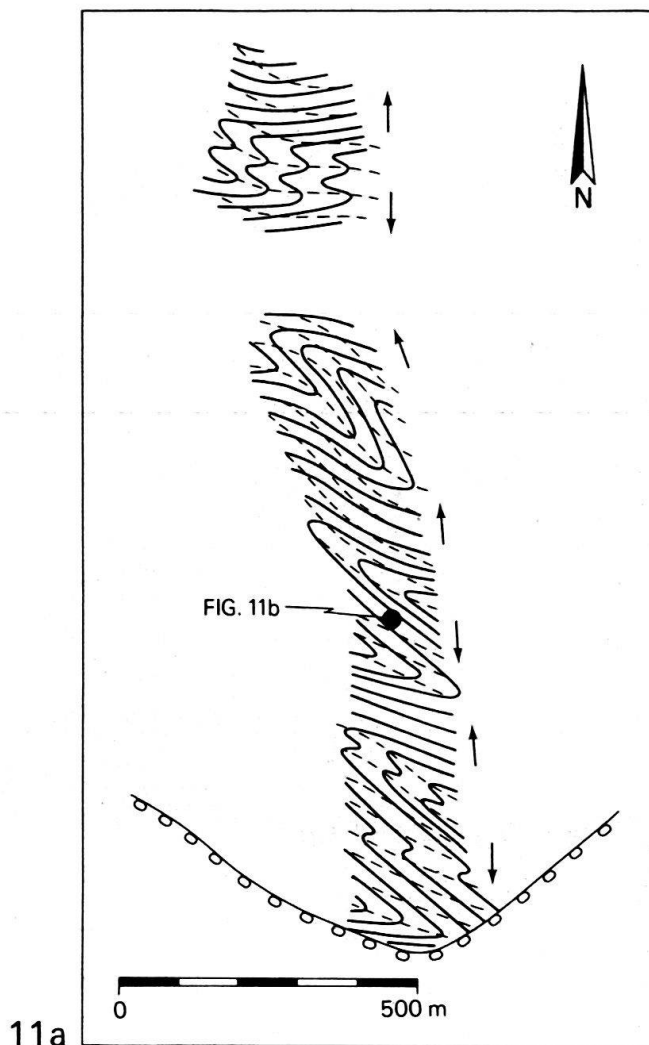
folds showing a Z-shape asymmetry. This very open aspect of the folds in the horizontal plane is caused by the gentle overall plunge of the D_{V4} structures towards the east. In profile they appear to be rather tight. The folds are often, but not always, cut by a steep (usually north dipping) D_{V4} axial plane cleavage. The northern boundary of the extent of D_{V4} deformation approximates a straight line, running E–W (i.e. parallel to the D_{V4} strike) along the northern border of the central part of the Orri dome (Fig. 7).

Quite a different situation occurs in the southeastern part of the dome (Fig. 7). Here mainphase axial planes dip towards the east instead of towards NNE as in the central area, so that the E–W strike of the D_{V4} axial planes is at large angles to sedimentary bedding and mainphase cleavage (Fig. 10). As a result, the axes of the D_{V4} folds plunge relatively steeply to the east. The strain related to D_{V4} folding has locally been rather large, as witnessed by the occurrence of very tight to isoclinal folds. The nature of these folds can easily be demonstrated by the frequently changing polarity of sedimentary bedding (Fig. 11).

The configuration of deformed mainphase cleavage traces (Fig. 7) and the distribution of structural elements in stereographic projection (Fig. 8 and 10), suggest that the mainphase and older folds in the presently exposed part of the Orri dome have been refolded into one large asymmetrical structure. The northern part of the dome represents,
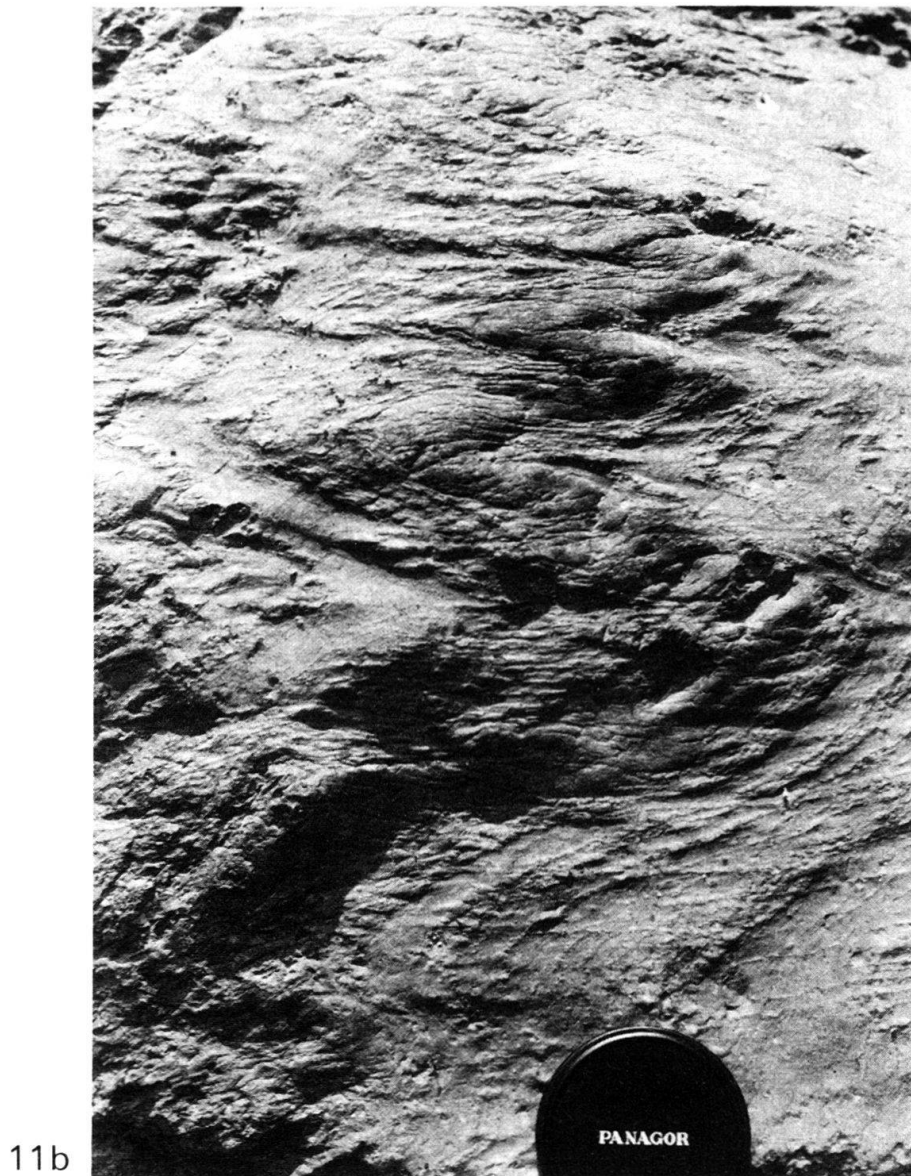
11b

Fig. 11. Very tight D_{V4} folds in the southeastern part of the Orri structure. For location see Fig. 7.
a) Form surface map of sedimentary bedding (thick lines) and D_{V4} cleavage in a river valley outcrop. The D_{V4} structures have been deformed by later D_{V5} and D_{PV1} deformation. Arrows indicate the facing direction of the beds. The Variscan folds are unconformably covered by Upper Carboniferous rocks in the southern part of the map.
b) Downward view on a sub-horizontal weathered surface in the river bed; east is towards the left. The D_{V4} cleavage planes and fold axes are very steep.

together with the southern limb of the Llavorsi syncline, the relatively undeformed long D_{V4} flank, whereas the central, southern and eastern parts are occupied by a composite D_{V4} short limb and fold-hinge area. In analogy with smaller-scale folds, the gentle eastward axial plunge of the large D_{V4} structure gives the impression that the fold system is much more open than it is in reality. The postulated southern long limb of the refolding structure is presently covered by post-Variscan rocks, which determines the minimum width of the fold-hinge area to be in the order of 12 km (Fig. 12). It will be shown in the chapter on post-Variscan deformation that the orientation of D_{V3} (and younger) cleavage has probably also been affected by later east-west shearing.
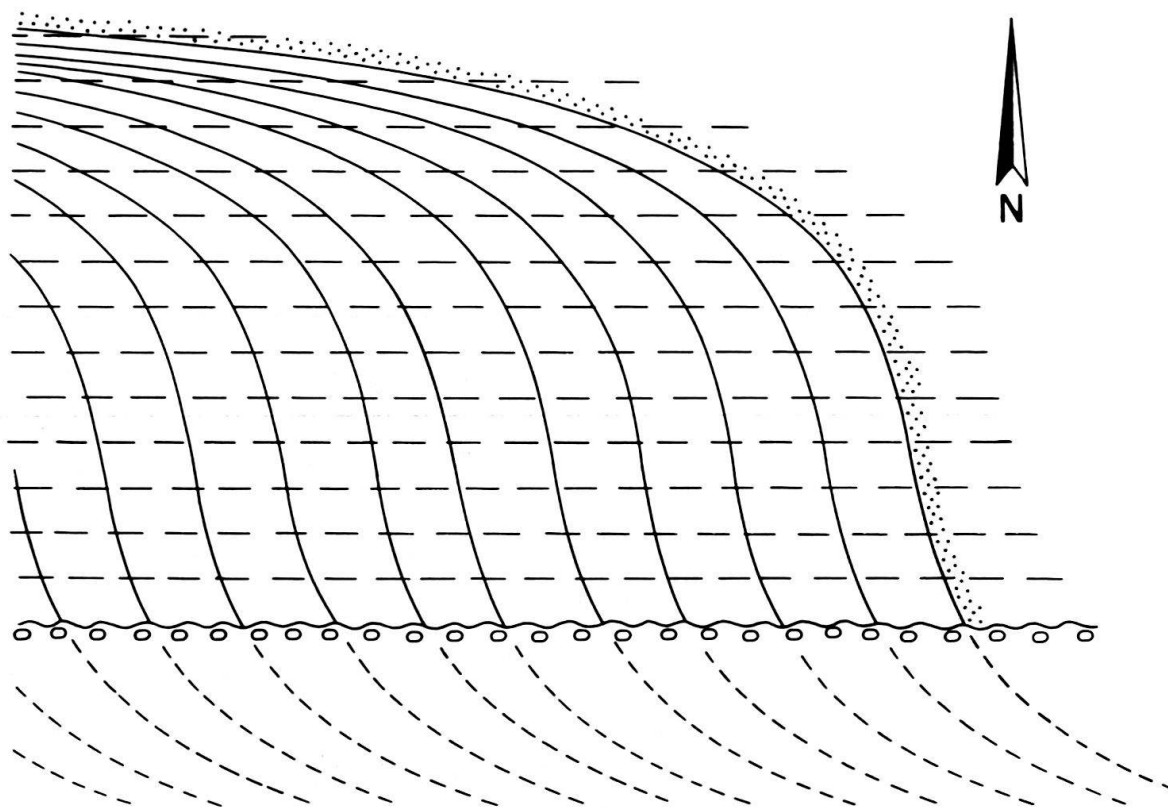
Fig. 12. Schematic map of the eastern part of the Orri dome showing folded D_{V3} cleavage, east-west striking D_{V4} cleavage, and the Variscan unconformity. The orientation of the D_{V3} cleavage changes from north dipping in the north to east dipping in the east (and probably north again below the unconformity). Compare with Fig. 7.

Second Variscan refolding (D_{V5})

Except for the long D_{V4} foldlimb along its northern edge, most parts of the Orri dome experienced a second Variscan refolding. D_{V5} folds do not occur very frequently in outcrop, but where observable they usually exhibit small amplitudes and wavelengths (cm–m scale). Cleavage development is restricted to the hinges of small-scale folds. Generally, the structures show a marked S-shaped asymmetry when looking north along the subvertical, N–S striking axial planes (an exception is shown in Fig. 13). In some areas of the Orri dome, D_{V5} deformation has affected older structural elements (e.g. D_{V4} cleavage, Fig. 14) on a larger scale. In such cases the D_{V5} cleavage is usually poorly developed.

The existence of still larger D_{V5} folds (up to km scale) can only be detected from deviations in trends of older cleavages (Fig. 7). In the southern half of the dome, large D_{V5} folds seem to occur rather frequently, but no foliation has developed, and folds are less tight than further north.

In many cases, D_{V5} folds are chevron-shaped, in particular the D_{V5} structures observed on outcrop scale. In addition, the folds may be very asymmetrical, giving them a kink-band-like appearance. For this reason, it is often impossible to distinguish in the field between kink-like D_{V5} folds and true kinkbands (see next section).
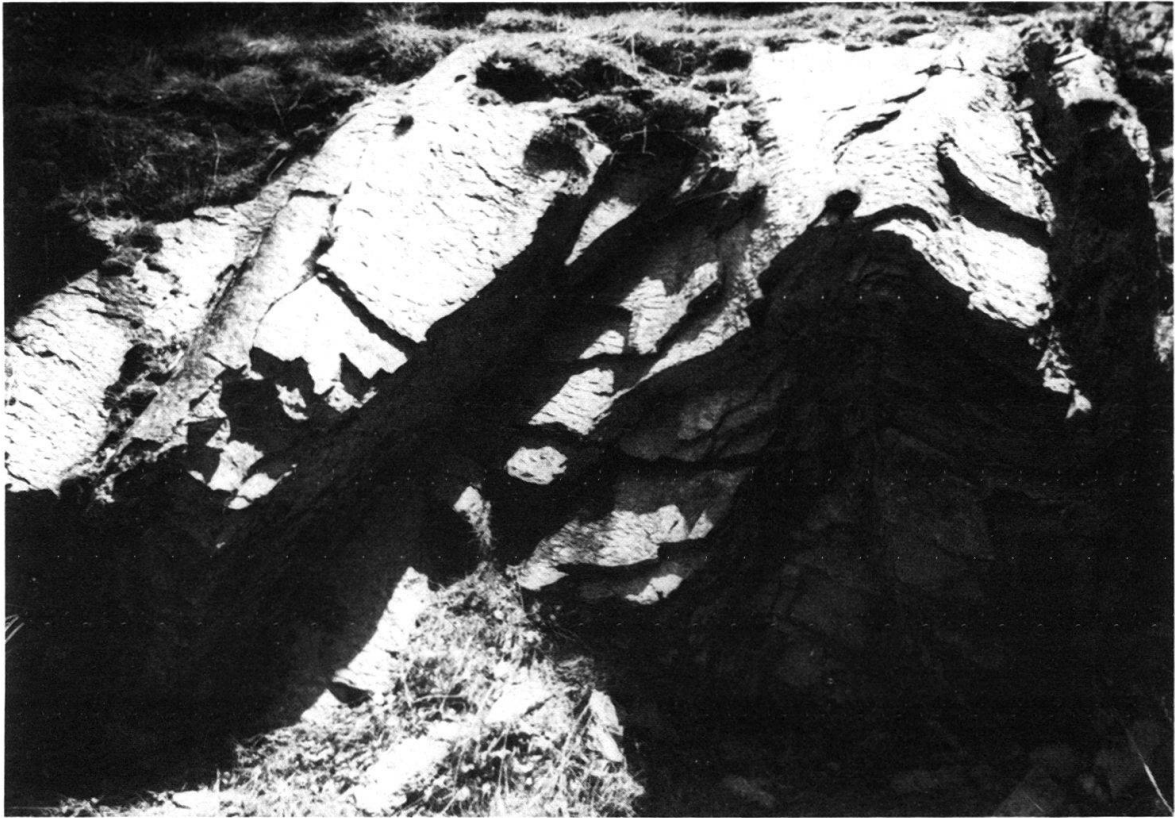
Fig. 13. Asymmetrical D_{V5} folds east of the Orri mountain (Fig. 7). This exposure shows the unique occurrence of D_{V5} folds on an overturned mainphase foldlimb; for this reason their asymmetry differs from what is normally encountered. View towards the south. Note that intersection lineations of sedimentary bedding and mainphase cleavage can be traced across the folds.
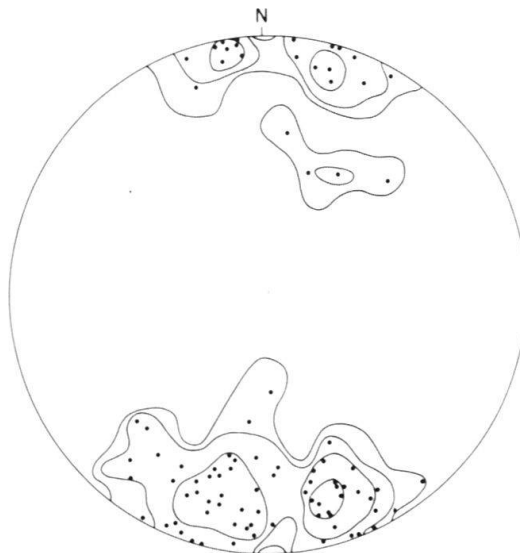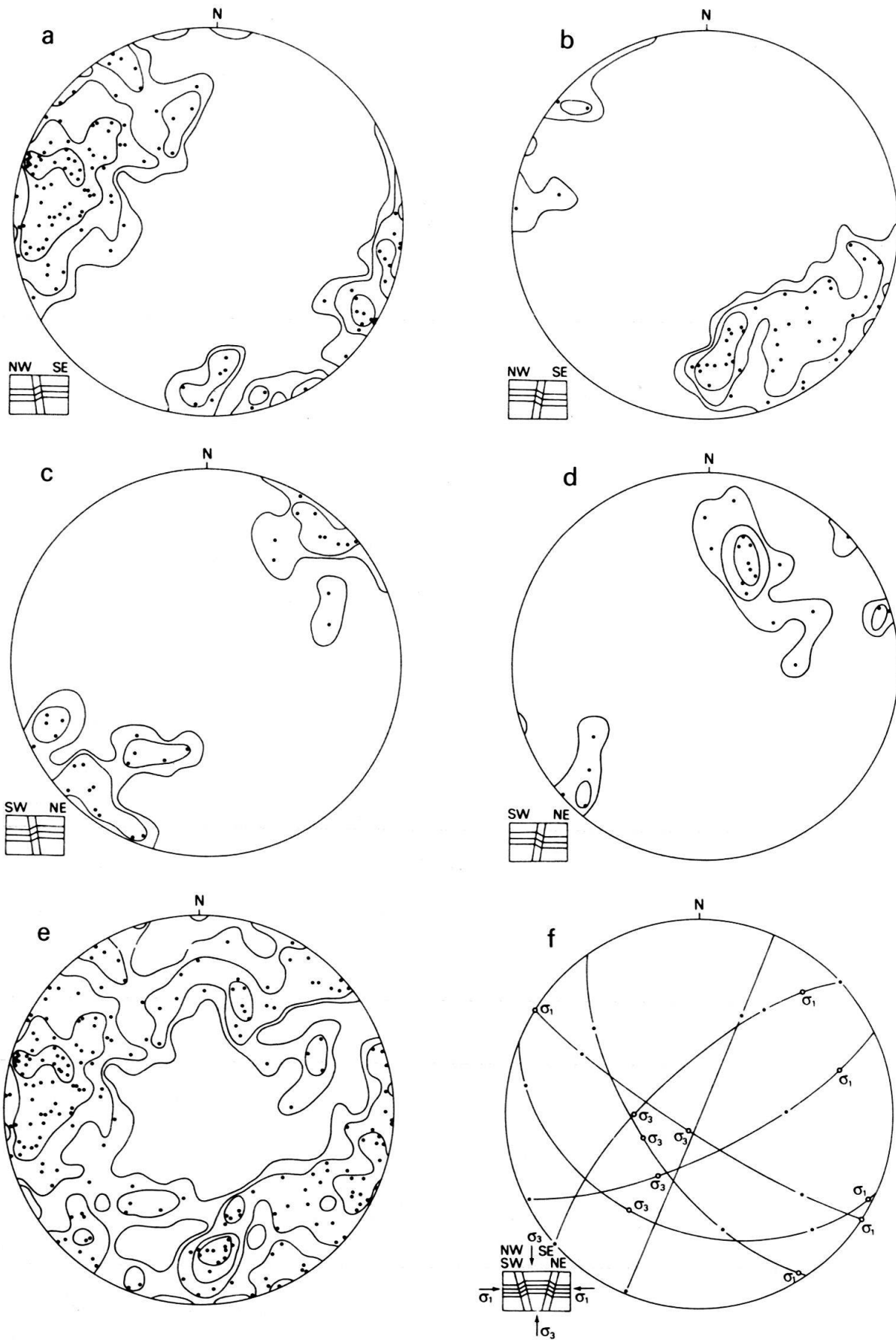

Fig. 14. Stereographic plot of poles to D_{V4} cleavage, slightly folded by D_{V5} deformation. The D_{V5} axial plane strikes N–S and is vertical, the fold axis of the very open chevron-type folds is vertical as well. For location see Fig. 7. Number of measurements: N = 90; contours represent 1, 2, 5, and 10 poles per 1% area (1.1, 2.2, 5.6, and 11.1% per 1% area).

Kinkbands of probable Variscan age (D$_{V6}$)

Kinkbands are not infrequent in the central part of the dome, where they are developed uniquely on (very) flat-lying long flanks of macroscopic mainphase folds. Their occurrence seems to be further restricted to finely laminated rocks in areas where no significant Variscan refolding has taken place and mainphase cleavage is poorly developed. Obviously, the distribution of the kinkbands has not only been governed by the direction and magnitude of the stress field in which they formed, but also by the presence of a strong anisotropy in the rock and its orientation with respect to the principal stresses.

The kinkbands are usually steep and most frequently strike NE–SW, or otherwise NW–SE (Fig. 15). The NE–SW kinks can be subdivided into two groups on the basis of their asymmetry: firstly a large group showing S-shaped asymmetry when looking NE (Fig. 15a), and, secondly, a group of kinks showing Z-asymmetry looking NE (Fig. 15b). As the kinkbands from these two groups predominantly dip towards SE and NW respectively, there is an obvious relationship between kink orientation and kink asymmetry, induced by the flattish attitude of the anisotropy (= lamination) plane. A similar, but less pronounced tendency can be observed regarding the dip angle of NW–SE striking kinkbands. The Figures 15c and d demonstrate that most of the NE dipping kinks have S-asymmetry, whereas the larger part of the SW dipping kinks have Z-asymmetry when looking NW.

The (very limited) occurrence of conjugate pairs of kinkbands (Fig. 16) further supports a relation between dip direction and asymmetry of the kinkbands. From the orientation of the conjugate kinks, the direction of the largest principal stress σ_1 can be easily reconstructed (RAMSAY 1962b; POWELL et al. 1985; Fig. 15f), indicating NW–SE and NE–SW subhorizontal compression (orthogonal to the strikes of the kinkbands). It is evident that σ_1 (and also σ_2) is at a low angle with the anisotropy plane (Fig. 15f). This appears to be a pre-requisite for kinkband development (DONATH 1969; WEISS 1969).

The kinkbands overprint Variscan mainphase folds, but have never been found to overprint younger Variscan structures. Nevertheless, the fact that kinks only developed on flat, non-refolded mainphase foldlimbs may be used as negative evidence that the

---

Fig. 15. Equal area stereographic projections related to D$_{V6}$ kinkbands in the central Orri dome. In the schematic profiles a horizontal anisotropy (bedding) plane has been chosen for convenience.

a) Poles to NE–SW striking kinkbands showing S-shaped asymmetry when looking NE. N = 112; contours represent 1, 2, 5, and 10 poles per 1% area (0.9, 1.8, 4.5, and 8.9% per 1% area.).

b) Poles to NE–SW striking kinkbands showing Z-shaped asymmetry when looking NE. N = 45; contours represent 1, 2, and 5 poles per 1% area (2.3, 4.4, and 11.1% per 1% area).

c) Poles to NW–SE striking kinkbands showing S-shaped asymmetry when looking NW. N = 32; contours represent 1 and 2 poles per 1% area (3.1 and 6.3% per 1% area).

d) Poles to NW–SE striking kinkbands showing Z-shaped asymmetry when looking NW. N = 21; contours represent 1, 2, and 5 poles per 1% area (4.8, 9.5, and 23.8% per 1% area).

e) Poles to all D$_{V6}$ kinkbands in the central part of the Orri dome. Note that part of the steep, east dipping planes may be axial planes to D$_{V5}$ chevron-type folds, as explained in the text. This diagram contains the combined data of Figs. 15a–d. Number of measurements: N = 210; contours represent 1, 2, 5, and 10 poles per 1% area (0.5, 1.0, 2.4, and 4.8% per 1% area).

f) Conjugate D$_{V6}$ kinkband sets in the central Orri dome. Plotted are poles to kinkbands (dots), planes containing poles to kinks (great circles), and the constructed orientations of the maximum (σ_1) and the minimum (σ_3) principal stress components related to kink formation (open circles). Note that σ_1 is horizontal in the case of NW–SE shortening (i.e. roughly parallel to the strike of mainphase structures), while it plunges 20°–30° along the gradient of long mainphase foldlimbs in the case of NE–SW shortening.
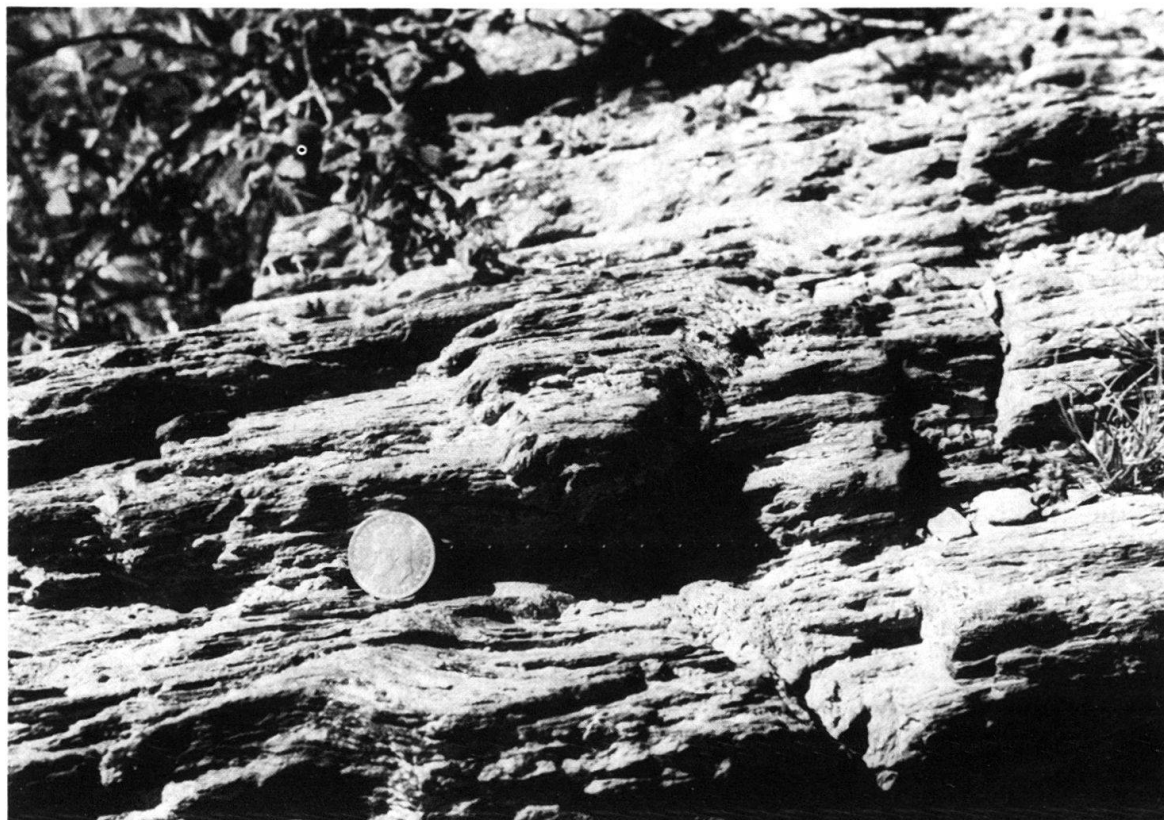
Fig. 16. Conjugate kinkbands, central Orri dome. View towards northeast. The kinks deform flat-lying sedimentary bedding on a long mainphase flank due to bedding-parallel compression. Location given in Fig. 7.

kinks are younger than D_{V4} and D_{V5}, as bedding was no longer flattish in areas affected by refolding, thus hampering kinkband development.

Deformation of the kinks themselves has not been observed in the Orri dome, so their minimum age cannot be established. We must herefore conclude that they may be of late Variscan or Alpine age. There are two reasons to assume that the former alternative applies:

Firstly, the kinkbands were formed by compression in the horizontal plane, in contrast to the kinks of probable Alpine age encountered in the south-eastern part of the dome (to be discussed later), that were generated by horizontal extension. This fundamental difference between the two types suggests different ages of deformation. A Variscan age for the "compressional" kinkbands is consistent with the overall compressional late Variscan evolution.

Secondly, there seems to be a genetic relationship between D_{V6} kinkbands and D_{V5} structures in the Orri dome. In the field it is often hard to distinguish between kink-like D_{V5} folds and true kinks. Still, D_{V5} axial planes tend to be very steep and strike N–S, whereas most D_{V6} kinks dip towards NE, SE, SW, or NW. It is well possible, therefore, that most of the steep N–S planes shown in Figure 15 do not represent true kinks but instead kink-like D_{V5} folds. The work of PATERSON & WEISS (1966) suggests that the genesis of kinks, conjugate folds and chevron-type similar folds can be closely related: whereas (conjugate) kinking is associated with a total shortening up to 10–25% (RAMSAY 1967), chevron folds can develop in the same anisotropic material when it is further shortened to roughly 50%.

This might explain the difficulty in separating D_{V5} and D_{V6} structures from each other in the field. Possibly there has been a gradual evolution from the development of "true" D_{V5} structures (macro- and meso structures, the latter with axial plane foliations), via chevron-type folding, to D_{V6} kinking, thus reflecting an overall decrease in horizontal shortening rate with time. This in turn probably reflects a drop in stress-level at the end of the Variscan orogeny. The magnitudes and directions of minor stresses will be relatively sensitive to local rock inhomogeneities. Therefore kinkbands may show a larger variation in orientation than D_{V5} folds (Figs. 14 and 15). Nevertheless, like second refolding structures, all observed kinkbands have a E–W component of shortening.

Kinkbands of similar nature as the D_{V6} kinks, encountered in other parts of the Axial Zone of the Pyrenees, appear to be overprinting D_{V5} structures (called F_4 by ZWART 1979), confirming their late Variscan age.

Post-Variscan deformation

The expression "post-Variscan deformation" is used here to refer to the Late Paleozoic (Stephanian and Permian) strike-slip and extensional deformation which took place directly after the Variscan orogeny had come to an end (SPEKSNIJDER 1987). It is hard or even impossible to completely distinguish post-Variscan deformation from Alpine deformation, just as it is difficult to assess the chronological order, if any, of post-Variscan events themselves. For this reason, the subdivisions used in this chapter are mainly of systematical nature and do not necessarily represent successive steps in the tectonic evolution of the Pyrenees.

Post-Variscan shearing (D_{PV1})

Figures 7 and 17 show that D_{V5} axial plane cleavages do not have constant orientations, but have consistently been bent towards the east (going from south to north) along approximately E–W to ESE–WNW trending zones. The deformation generation which caused this reorientation must be post-Variscan in age or younger (probably Stephano-Permian, see below), and is referred to as D_{PV1} deformation. It is postulated that this deformation took the form of east-west right-lateral shearing in the Orri dome.

Figure 17a shows the scatter in orientation of D_{V4} and D_{V5} cleavages in the southeastern part of the dome. The structural trend map of Figure 17b shows that the D_{V4} cleavage has been relatively little reoriented compared to the D_{V5} cleavage, although D_{V4} cleavage has been slightly folded around steep N–S axial planes during D_{V5} deformation. This observation is taken to indicate that the younger cleavage was more susceptible to shearing, as a function of its orientation, than the older cleavage. The fact that D_{V4} cleavage traces have seemingly been little affected by D_{PV1} deformation, suggests that post-Variscan shearing might have taken place along and parallel to the D_{V4} cleavage planes; i.e. in E–W to ENE–WSW direction with right-lateral sense (Fig. 17b).

The impact of post-Variscan shearing on mainphase structures is more difficult to establish, as folding of the D_{V3} cleavage may result from the combined effects of the D_{V4}, D_{V5}, and D_{PV1} deformations (the effect of D_{V6} deformation on mainphase cleavage is negligible). Figures 18a–c show the distributions of D_{V3} cleavage for a number of sub-areas in the Orri dome. Although the spread of data is limited, the distributions define partial great circles and therefore apparent foldaxes for the combined effects of post-mainphase deformation. In the case of Figure 18a it appears that mainly D_{V4} folding must
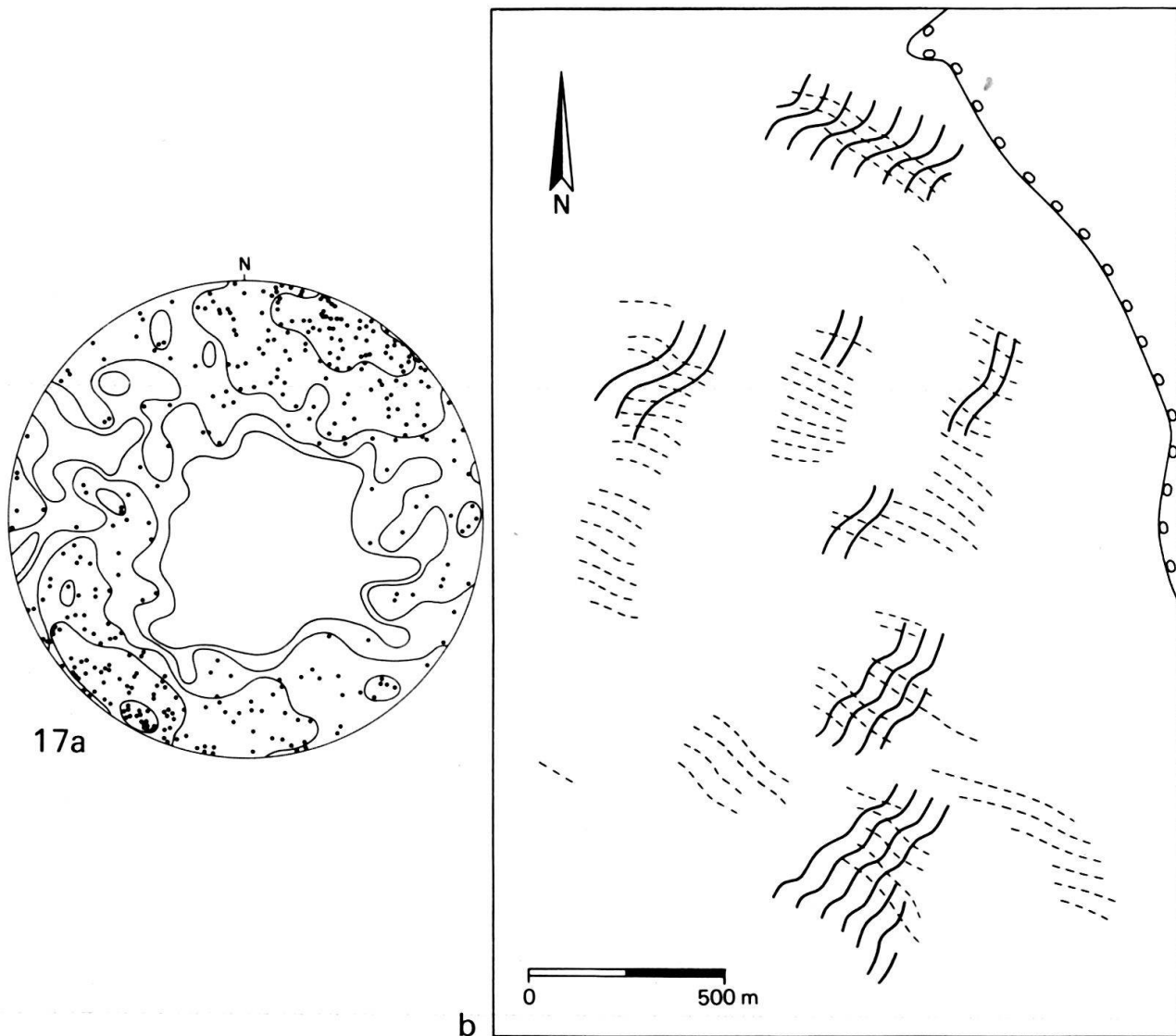
Fig. 17. Redistribution of D_{V4} and D_{V5} cleavages in the southeastern Orri dome (Fig. 7), caused by post-Variscan shear. Poles to D_{V3} cleavages from the same area are shown in Figure 10.
a) Equal area stereographic projection of poles to D_{V4} cleavage (NNW–SSE to ENE–WSW strike), and poles to D_{V5} cleavage (N–S to NE–SW strike). In this projection no attempt has been made to strictly distinguish between the two cleavages, as discrimination between the two on the basis of their orientation is also difficult to make in the field. Number of measurements: N = 366; contours represent 1, 2, 5, 10, and 20 poles per 1 % area (0.3, 0.5, 1.4, 2.7, and 5.5% per 1% area).
b) Simplified structural trend map showing deformed D_{V5} (continuous lines) and D_{V4} (dashed) cleavages. Upper Ordovician formations crop out in the upper right part of the map. Note the relatively strong reorientation of D_{V5} cleavage (consistent with right-lateral shear).

be held responsible for mainphase cleavage reorientation, but the other two redistributions cannot be easily attributed to Variscan refolding. If the apparent foldaxes of these and other areas are plotted together in a stereographic projection (Fig. 18 d), it turns out that they define a great circle and thus lie in one plane. Redistribution of lineations, such as foldaxes, in a plane may suggest that the (latest) deformation has been of the simple shear type (RAMSAY 1967, chapter 8). If so, the slip direction will be defined by the intersection line between the lineation distribution plane and the shear plane (HOBBS et al.
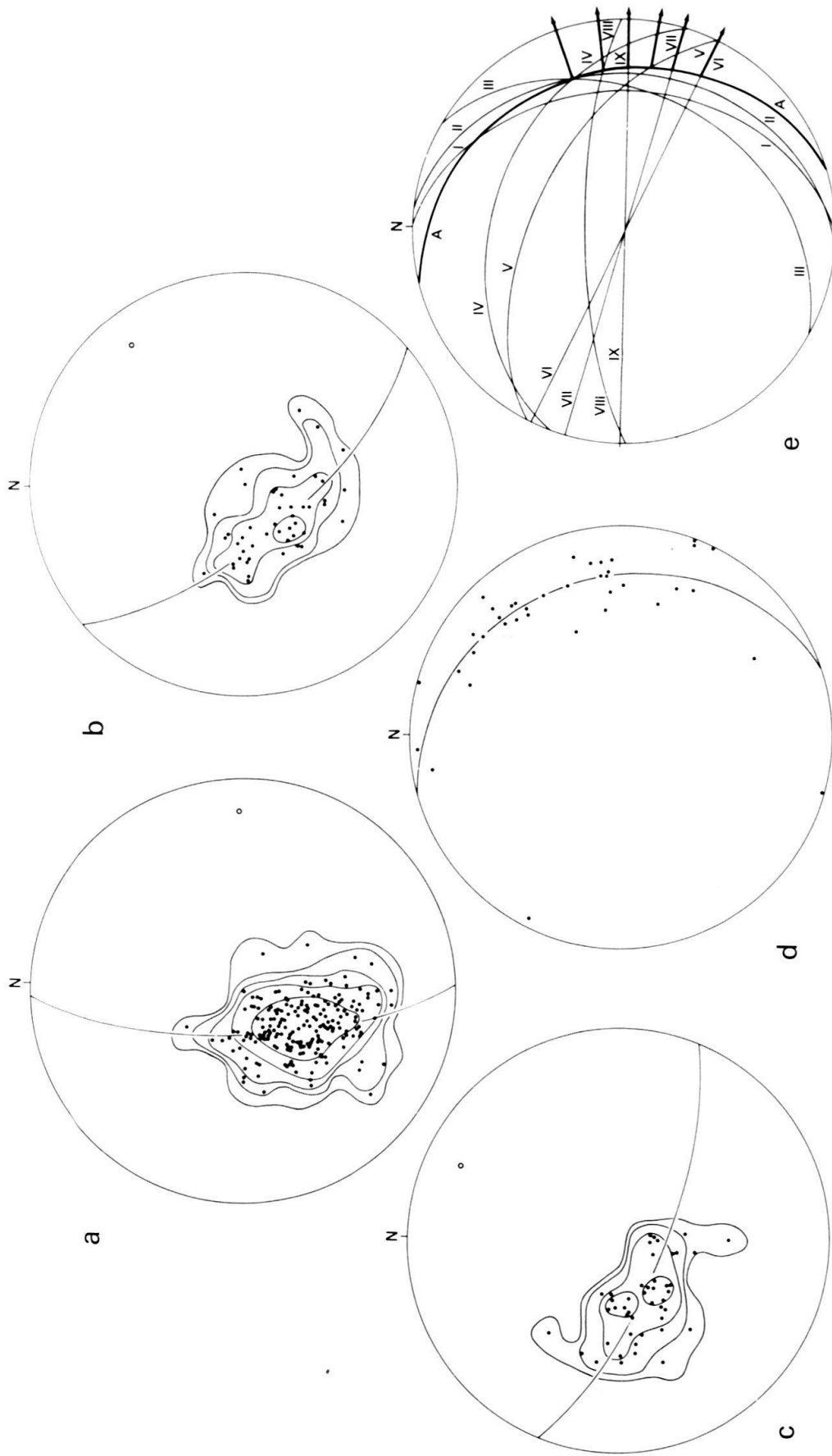
Fig. 18. Reorientation of Dv_3 cleavage as a result of later Variscan, and, in particular, Dpv_1 deformation. Locations shown in Figure 7.

a) Poles to mainphase cleavage in the north-central part of the dome. The position of the (apparent) fold axis is indicated by the open circle. This diagram is identical to Fig. 8a. Number of measurements: N = 195; contours: 1, 2, 5, 10, and 25 poles per 1% area (0.5, 1.0, 2.6, 5.1, and 12.8% per 1% area).

b) Poles to mainphase cleavage, and fold axis; central-east Orri dome. N = 45, contours: 1, 2, 5, and 10 poles per 1% area (2.2, 4.4, 11.1, and 22.2% per 1% area).

c) Poles to mainphase cleavage, and fold axis; northeastern Orri dome. N = 46; contours 1, 2, 5, and 10 poles per 1% area (2.2, 4.3, 10.9, and 21.7% per 1% area).

d) Apparent fold axes of mainphase cleavage from 38 subareas in the Orri dome, including the axes shown in Figures 18a–c. The great circle represents the redistribution plane of the foldaxes.

e) Dpv_1 shear directions (indicated by heavy arrows), found as intersection lines between possible shear (anisotropy) planes and the redistribution great circle shown in Fig. 18d. Great circles represent the following planes: (A) Foldaxes redistribution plane; (I) Thrustplanes in the eastern part of the Orri dome (HARTEVELT 1970); (II) Average mainphase cleavage orientation northeastern part dome, N = 107; (III) Average mainphase cleavage orientation in a subarea in the southwest, N = 11; (IV) Average mainphase cleavage orientation in the area of Fig. 3, N = 141; (V) Average mainphase cleavage orientation in the area of Fig. 4, N = 52; (VI) Average Dv_4 cleavage orientation from Fig. 20b, N = 62; (VII) Reorientation direction Dv_5 cleavages (see text); (VIII) Average orientation Dv_4 cleavages area Fig. 14, N = 90; (IX) Strike Alt Segre fault (SOLE SUGRAÑES 1978) and faults La Seu Basin (SPEKSNIJDER 1985).

1976; p. 192). Figure 14 demonstrates that reorientation of D_{V5} cleavages takes place along E–W to ESE–WNW striking planes. In addition, the fact that D_{V5} axial planes do not significantly change in dip-angle in Figures 14a and 17a, suggests that D_{PV1} apparent foldaxes may be subvertical.

Event though unambiguous proof is lacking, it seems justified to postulate, after combination of all observations, that steep E–W to ESE–WNW striking planes acted as probable shear planes for the D_{PV1} shear deformation. The slip vector can then be established to be slightly E to ESE plunging for the central and eastern parts of the Orri dome (Fig. 18e). The sense of the shear movement was most likely right-lateral, as suggested by Figures 12 and 17b.

All rocks in the Orri dome are mechanically strongly anisotropic due to the fine sedimentary lamination and the presence of several penetrative foliation planes. When favourably oriented with respect to the slip direction, existing anisotropy planes can have taken up much or all of the shear movement. This might apply to the ESE–WNW striking mainphase cleavage (except when it is strongly folded), and in particular to the steep E–W striking D_{V4} cleavage. Cleavage-parallel movement on these planes might explain why D_{V4} cleavage sometimes appears to be undeformed on a large scale. Structural elements that make large angles with the shearing direction, such as D_{V5} cleavage, could not take up any cleavage-parallel movement, but became folded instead. Similarly, it may be argued that the regional folding of mainphase cleavage in the eastern part of the Orri dome (Fig. 12) was initially caused by D_{V4} deformation, whereas the structure was later tightened by D_{PV1} shearing. The shear direction is in this case parallel to gently east dipping thrusts along the eastern border of the dome (HARTEVELT 1970), which suggests that these structures are of post-Variscan age as well.

Further independent observations substantiate the idea that important E–W directed shearing and faulting may have taken place in the Orri dome. SPEKSNIJDER (1985) demonstrates the existence of synsedimentary strike-slip fault zones along east-west directed Stephanian and Permian basins which unconformably overlie the Orri dome in the south. Large-scale post-Variscan divergent strike-slip movements (SPEKSNIJDER 1987) resulted in the formation of an elongated, narrow sedimentary basin with a complex internal organisation. The maximum sediment thickness (approximately 1500 m), the length and width of the basin (more than 50 km and 5 km respectively), and the occurrence of thick sequences of tuffs and andesitic basalts indicate that the basin developed above a major fault zone which must reach deep into the crust. It can be shown that the strike-slip movement along the fault zone must have been right-lateral; the minimum horizontal displacement appears to have been in the order of 10–20 km (SPEKSNIJDER 1985).

Upper Carboniferous and Permian rocks which were affected by this strike-slip faulting have been tilted, together with the Variscan unconformity plane and the under-lying Variscan rocks, to a dip of approximately 45° to the south during Tertiary uplift (to be discussed later). It follows that the rocks of the Orri dome, which now crop out to the north of the Upper Paleozoic sedimentary basins, must have been more or less underlying these basins before Alpine tilting took place.

Thus a relationship can be established between superficial E–W post-Variscan syn-sedimentary strike-slip brittle failure, and semi-brittle right-lateral shear in the Variscan basement. East-west right-lateral movements along the Pyrenean Variscan mobile belt

probably played an important role throughout the Paleozoic (SPEKSNIJDER 1987). Post-Variscan dextral strike-slip movements in the Pyrenees and the rest of southern Europe have been attributed to plate-scale shearing between the Urals and the Appalachians by ARTHAUD & MATTE (1977).

Post-Variscan cleavage fanning (D_{PV2})

The gradual decrease of mainphase cleavage dip towards the south (Fig. 7) reflects part of the so-called cleavage fanning in the Axial Zone of the Pyrenees (ZWART 1979). Whereas mainphase cleavages are subvertical in the northern part of the axial zone, they dip north and flatten in a southern direction (ZANDVLIET 1960; MULLER & ROGER 1977). The significance and timing of the cleavage fan formation has been a matter of dispute: some authors attribute the fanning to late-Variscan horizontal N–S extension (ZWART 1979, 1981), others to both late-Variscan and Alpine warping of an originally steep cleavage (MULLER & ROGER 1977). MEY (1968) and many French authors (see ZWART 1981) claim that the foliations of the Axial Zone were originally formed in a horizontal position. The present writer agrees with ZWART (1981), that the latter hypothesis seems unlikely.

As will be shown later, most of the warping of the Variscan cleavage, in particular along the southern rim of the Orri dome, can be attributed to Alpine deformation. Nevertheless, part of the fanning can result from post-Variscan extension (SPEKSNIJDER 1987), rather than from late Variscan extension as envisaged by ZWART (1979), as no further indications for extension of that age can be found. The strain related to extension could have been distributed along cleavage parallel normal faults leading to outward rotation of the cleavage planes. Such a rotation in the vertical plane as a result of post-orogenic relaxation has already been proposed by HOEPPENER (1955) for the Rhenic slate belt. Correlation problems across the mainphase folds of the northern Orri dome led SPEKSNIJDER (1987, Fig. 4) to postulate cleavage-parallel normal faults, similar to those envisaged by ZANDVLIET (1960). As cleavage-parallel movement will not allow the cleavage planes to rotate through the horizontal, the south dipping attitude of the mainphase cleavage in the southernmost part of the Orri dome must be attributed to another mechanism, i.e. Alpine thrusting.

Kinkbands of probable post-Variscan age (D_{PV3})

Kinkbands encountered in the southeastern part of the dome are of different nature than the previously described D_{V6} kinks. They overprint a very steep penetrative D_{V4} axial plane cleavage, which only occurs as a dominant cleavage in this part of the dome. D_{PV3} kinks were generated as a result of N–S extension in the horizontal plane, as witnessed by the often occurring conjugate sets of kinkbands (Fig. 19 and 20 a). This in contrast to the D_{V6} kinks, which were formed by horizontal east-west directed compression. Also in this case, the largest principal stress component is roughly parallel to the anisotropy (cleavage) plane (Fig. 20 b and c).

The age of the kinks cannot be established with certainty. They overprint D_{V4} cleavage, and as they were generated by N–S extension, they are possibly of post-Variscan age. They could, on the other hand, also be related to Alpine vertical uplift and horizontal

Fig. 19. Conjugate kinkbands (generated by horizontal extension) deforming steep D_{V4} cleavage in the southeastern Orri dome. North is towards the left. Position in Fig. 7.

extension. The fact that D_{PV3} kinks have not developed in the Stephanian tuffs directly overlying the Variscan rocks does not necessarily indicate a pre-Stephanian age of formation, but instead must be attributed to the lack of a penetrative fabric within the massive tuffs. Figure 20c shows orientation data of kinkbands, maximum principal stress directions related to conjugate kinks, and D_{V5} cleavages, projected on a vertical NNE–SSW plane which runs parallel to the measured structural profile. It can be seen from this diagram that kinks are only present in an area where the dip of the pre-existing D_{V5} cleavage changes rapidly (between 0–1 km from the unconformity). This may suggest that kinkband development and change in cleavage attitude are closely related, but on the

Fig. 20. Orientation and geometry of D_{PV3} kinkbands in a NNE–SSW profile; southeastern part of the Orri dome. See Fig. 7.

a) Poles to kinkbands. Open circles represent constructed σ_1 directions related to the development of six conjugate kink sets (c. f. Fig. 15 f). The great circle indicates the vertical NNE–SSW plane on which data have been projected in Figure 20 c. Number of measurements: N = 45; contours: 1, 2, and 5 poles per 1 % area (2.2, 4.4, and 11.1 % per 1 % area).

b) Poles to D_{V5} cleavage in the same profile. The great circle represents the projection plane of Figure 20 c. Note that reconstructed σ_1 directions (open circles) approximately lie within the (averaged orientation of the) cleavage plane. Contours: 1, 2, and 5 poles per 1 % area (1.6, 3.2, and 7.7 % per 1 % area).

c) The data of Figures 20 a and b projected upon a 25°–205° striking vertical plane, parallel to the measured section. In this diagram (two-dimensional) orientation data are plotted as a function of their distance to the Variscan unconformity plane towards the south. Diamonds: dip of D_{V5} cleavages; heavy dots: σ_1 orientations of conjugate kinks; open circles: dips of kinkbands. For discussion see text.

a

b

c
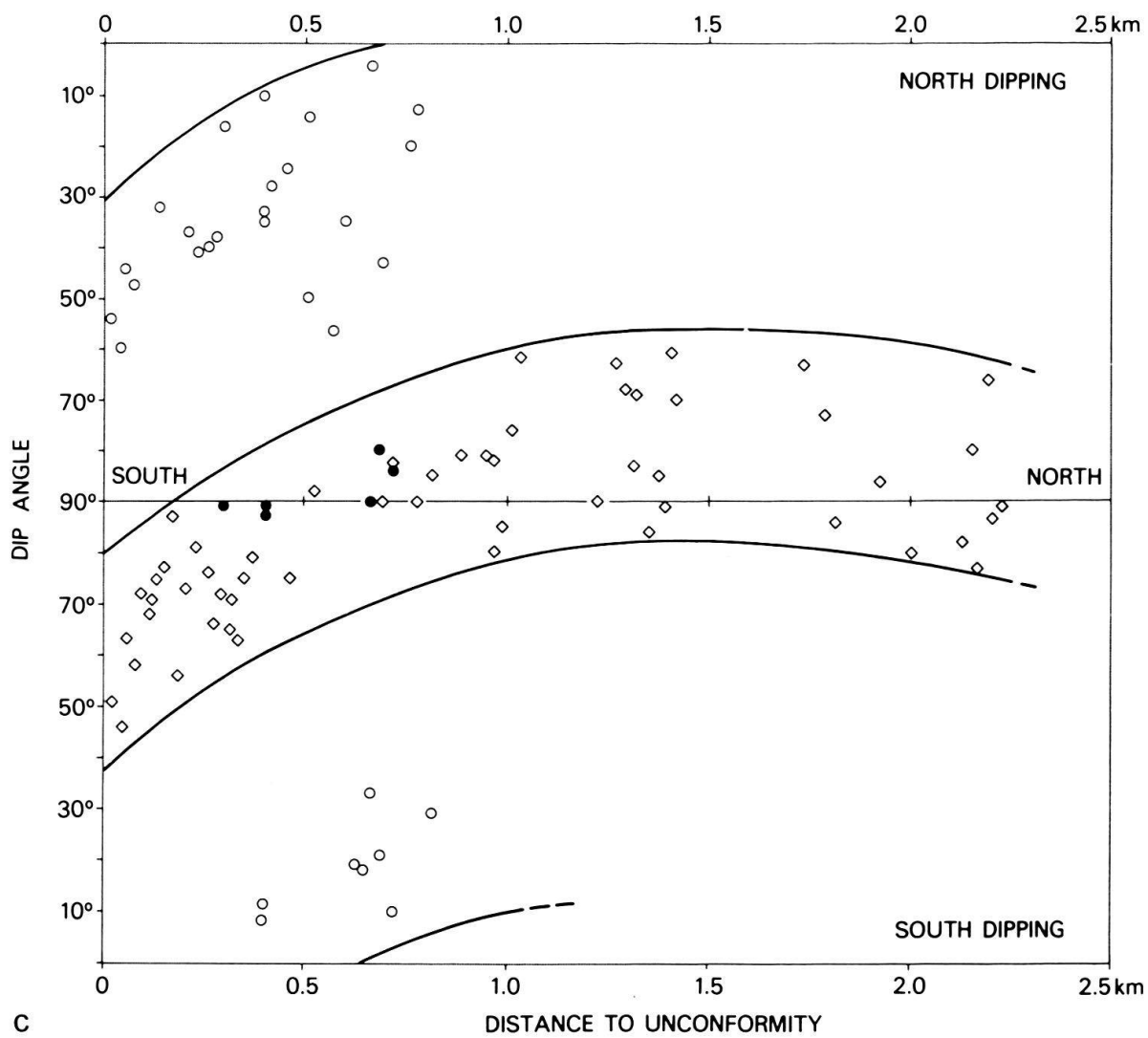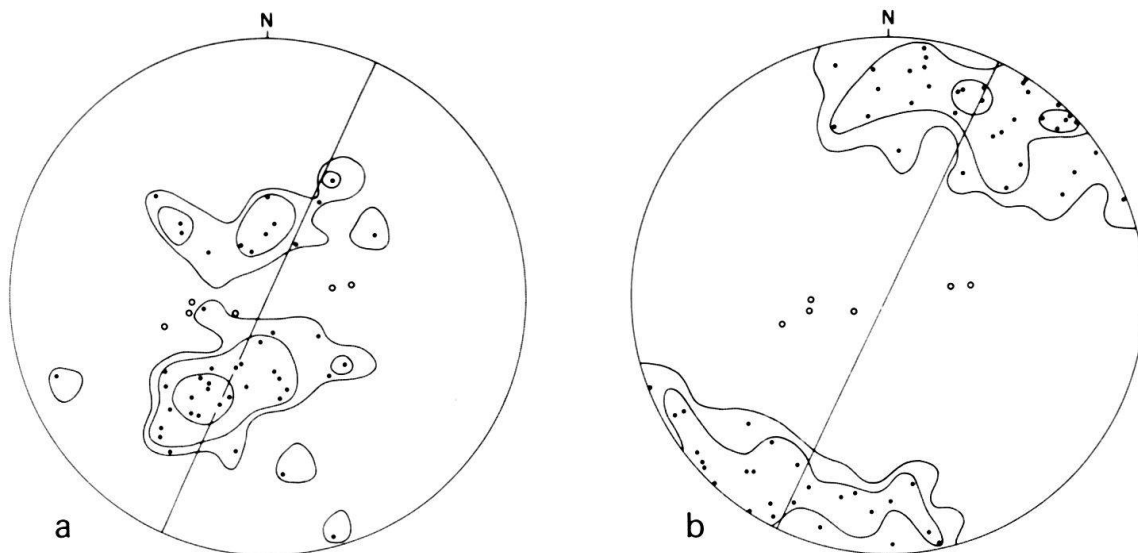
other hand the diagram reveals that the kinks experienced exactly the same rotation in the vertical plane as the cleavages. In other words, the kinks must have developed in an extensional regime which did not affect cleavage dips significantly, to become rotated together with the cleavage planes during later deformation. For this reason, kinkband development and subsequent rotation are tentatively attributed to post-Variscan and Alpine deformation, respectively.

Alpine deformation

There has been much debate in the literature concerning the influence of deformation of Alpine age in the Axial Zone. While the impact of Alpine deformation was originally thought to be restricted to the Tertiary uplift of the Axial Zone as a whole (c.f. ZWART 1968), it was already known that Alpine thrusts may cut deep into the Variscan (DE SITTER 1965). SEGURET (1970) demonstrated the existence of major Alpine nappe systems south of the Axial Zone (involving pre-Stephanian rocks in the Nogueras Zone). More recently WILLIAMS & FISCHER (1984) and WILLIAMS (1985) presented their reconstructions of balanced sections across the Pyrenean belt, based on the assumption of thin-skinned thrusting affecting the whole of the Axial Zone, as well as the southern foreland.

The development of mylonitic shear zones of Alpine age in the Variscan has been discussed, amongst others, by LAMOUROUX et al. (1981).

In the Orri dome, no reliable overprinting relationships are available to establish the sequence of Alpine and post-Alpine deformational events, especially because they have been of brittle nature. Comparison with surrounding areas suggests that thrusting is of Eocene age (SEGURET 1970), while normal and oblique-slip faulting on various scales occurred during the post-Alpine period, offsetting rocks up to Pliocene age.

Alpine thrusting (D_{A1})

The Orri dome is surrounded by thrusts of proven or probable Alpine age. In the south, a complicated allochthonous unit called the Nogueras Zone (SEGURET 1970), has been emplaced on Keuper evaporites which almost directly overlie the Orri dome unconformably (Fig. 2). Towards the north, the dome is cut-off by the Llavorsi fault, which might be of Alpine age (ZWART 1979), whereas a number of thrusts to the west of the Orri dome are definitely of Alpine age (MEY 1967 b, 1968).

Along the southwestern edge of the Orri structure, a major river cuts deeply into Cambro-Ordovician rocks (topographic relief more than 1700 m). At the bottom of the river valley, flat-lying Keuper evaporites are exposed, which seemingly underlie Variscan rocks (Fig. 2). This observation suggests that (this part of) the dome is allochthonous as well, emplaced on a décollement level within the Triassic evaporites. Alpine low-angle faults along which Variscan rocks have been thrusted southward over younger rocks are known from many other localities along the border of the Axial Zone (PARISH 1984; MUÑOZ et al. 1986).

The details of nappe tectonics in and around the Orri dome appear to be complicated and largely fall beyond the scope of this paper. Nevertheless, a short resume will be given of the published literature on the subject, and a conceptual cross-section will be presented which might explain the important change in cleavage attitude from north to south in the Variscan.
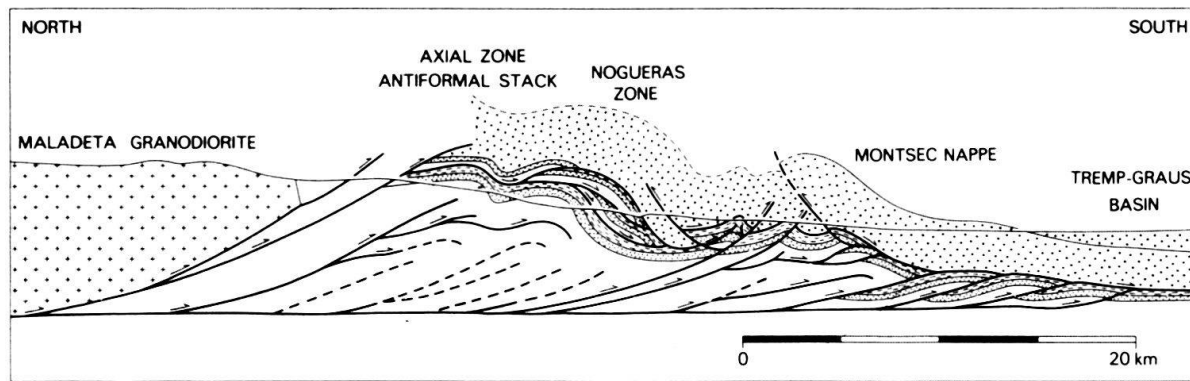
Fig. 21. Structural cross section through the south-central Pyrenees, west of the Orri dome (modified after WILLIAMS 1985, with permission of the author). Ornamentation represents intrusive Variscan rocks (crosses), Permo-Triassic redbeds (dense dots), Keuper evaporites (parallel lines) and undifferentiated Mesozoic and Tertiary sedimentary rocks (large dots). Non-intrusive Variscan rocks have been left unornamented. The main décollement plane is located within the Keuper evaporites (N. B.: The thickness of the strongly deformed Keuper evaporites is somewhat exaggerated in this section).

Palinspastic reconstruction of balanced sections west of the Orri dome (WILLIAMS & FISCHER 1984, WILLIAMS 1985) indicates that thrusting cannot have been restricted to movements concentrated within the Keuper evaporites alone, but instead a number of duplexes must have developed in the southern Axial Zone (Fig. 21). All thrusts are supposed to join downward in a sole thrust within the Variscan basement. The strong southward dip of the Variscan unconformity and thrust planes along the Nogueras Zone
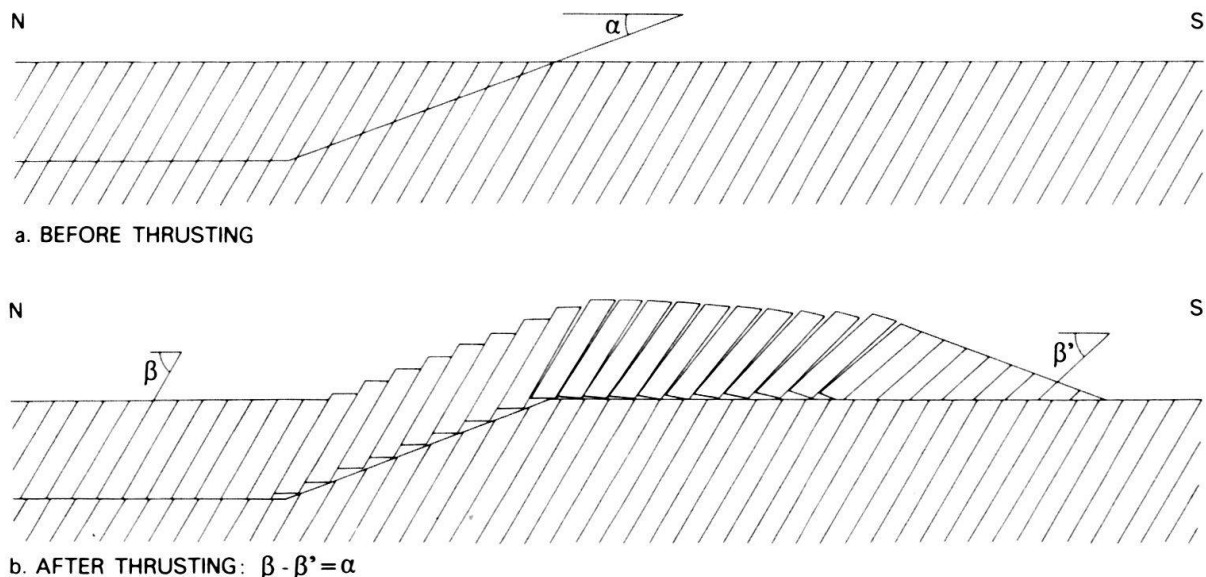

Fig. 22. Schematic diagram showing the variation of cleavage attitude as a result of thrusting within strongly anisotropic rock. The orientation of cleavage planes above the ramp may remain approximately parallel to their original orientation due to cleavage-parallel slip. A strong decrease of cleavage dip will occur above the flat; the maximum rotation angle $(\beta-\beta')$ is equal to the dip α of the ramp. If a ramp would develop parallel to the anisotropy plane, the cleavage in the southern part of the thrusted unit would be subhorizontal. Cleavage dips towards the south, however, could never occur in the configuration shown here, even if substantial post-Variscan cleavage fanning (D_{PV2}) had taken place. A strong foreland dip of the thrustplane is therefore required to rotate cleavage planes through the horizontal, as shown in Figure 23.

can be elegantly explained by antiformal stacking below the southern part of the present-day Variscan outcrop. A similar structural configuration (although on a smaller scale), has been described by Muñoz et al. (1986), from outcrops in the Freser valley, 50 km east of the Orri dome.

The variation in mainphase cleavage dip can be attributed to three effects. Firstly, post-Variscan cleavage fanning (D_{PV2}) may have caused an initial decrease of cleavage dip towards the south before Alpine thrusting took place, or, alternatively, Variscan cleavage may not have developed with uniform orientation during orogenesis. Secondly, cleavage attitude could have been affected by the flat-ramp geometry of thrust units as shown in Figure 22. Thirdly, a foreland (southward) directed tilt of the thrust system due to anticlinal stacking will equally impose a southward tilt on Variscan structures as conceptually shown in Figure 23. Note that this section is only intended as an illustration of the possible thrust geometry and cannot be palinspastically reconstructed.

The position of the postulated roof-thrust is related to cleavage attitude: steep co-planar in the north, and decreasing in dip towards the south. If this interpretation is correct, the thrust should also have developed towards the east over at least some distance in the Orri dome. The monotonous nature of the Cambro-Ordovician rocks does not allow the location of structural contacts, but it is striking that the northern limit of Variscan refolding (D_{V4} and D_{V5}) seems to be more or less coincident with the boundary between tilted and co-planar cleavage planes (Fig. 7). Obviously, the occurrence of
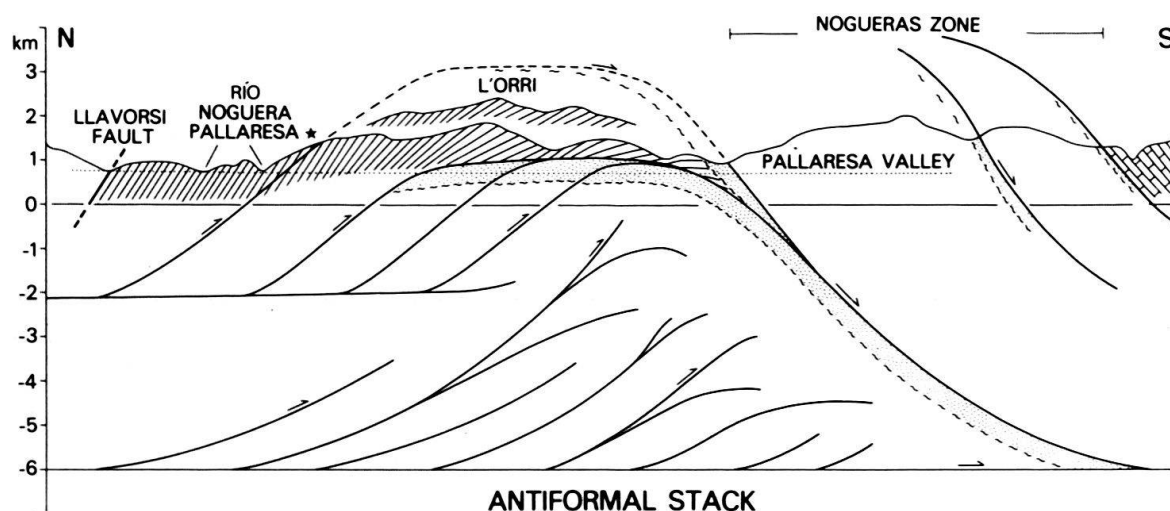

Fig. 23. Conceptual cross-section through the western part of the Orri dome (profiles over the top of the Orri mountain and along the valley of the Rio Noguera Pallaresa have been projected), and the northern part of the Nogueras Zone. Location shown in Fig. 2. The point at the surface which marks the southern limit of coplanar mainphase cleavage (shown by an asterisk), is taken to indicate the position of a roofthrust to an emplaced unit which is mainly composed of Cambro-Ordovician rocks. In this interpretation the roofthrust joins with the southward dipping thrustplane that forms the northern boundary of the allochtonous Nogueras Zone. The foreland dip of this plane is attributed to antiformal stacking as suggested by WILLIAMS (1985); see Fig. 21. The large outcrop of the Keuper evaporite in the Noguera Pallaresa valley (4.5 km in N–S direction), combined with its restricted undisturbed maximum thickness (some hundreds of meters), suggests duplex development below the Orri thrust unit. As the details of thrust configuration in the Nogueras Zone are not known, and as the nature and age of the latest movement on the Llavorsi fault is unclear, the section is not balanced and no attempt has been made to reconstruct it. Ornamentation represents cleaved Cambro-Ordovician; undifferentiated Paleozoic rocks (white); (Permo-) Triassic including Keuper evaporites (dotted); and Mesozoic limestone (southernmost part of the profile). Horizontal and vertical scales are equal.

Variscan refolding and mainphase cleavage reorientation can be closely related, but an alternative is that the postulated Alpine thrust now juxtaposes two different Variscan structural units (with and without refolding) which were previously separated from each other. Based on this reasoning, the tentative trace of the thrust under discussion is shown as a heavy dashed line in Figure 7.

Post-Alpine deformation

Post-Alpine deformation is defined to incorporate all (brittle) deformation which took place after the main Alpine (or Pyrenean) compressional event. Its occurrence is therefore restricted to the Neogene and the Quarternary.

Post-Alpine faulting (D_{PAl})

South of the Orri dome, numerous east-west steep normal faults with throws up to some meters are found in Permian and Triassic redbeds, usually involving a downthrown northern block.
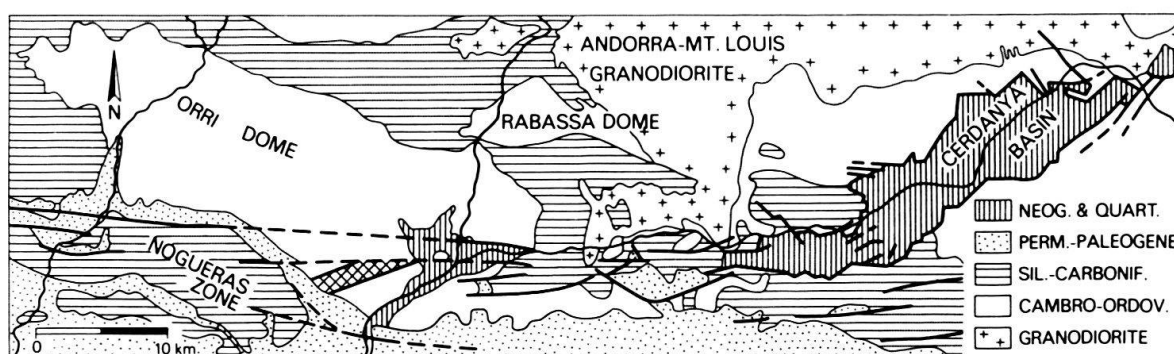

Fig. 24. Faults of proven or probable post-Alpine age, together forming a complicated E–W striking oblique-slip system along the southern boundary of the Axial Zone of the Pyrenees. The part east of the Orri dome has been named the Alt Segre fault by SOLE SUGRAÑES (1978). The cross-hatched area in the southern Orri dome represents a major overturned mainphase (D_{V3}) foldlimb which is abruptly cut-off in the north. "Permian-Paleogene" in the legend to the figure includes Westphalian D and Stephanian rocks. Fault traces mainly after ZWART & ROBERTI (1976), HARTEVELT (1970) and BROUWER (1968); structural outline of the Cerdanya Basin after GOURINARD (1971).

The same sense of movement has been recorded on an east-west striking fault which offsets Miocene and younger rocks in the eastern part of the dome. Along strike towards the east, a complicated fault system, named the Alt Segre fault by SOLE SUGRAÑES (1978), affects Eocene and older rocks including Variscan basement (Fig. 24). The dip-slip offset on the Alt Segre fault (northern block downthrown) may be a kilometer or more (HARTEVELT 1970). The existence of a possible strike-slip component of movement can be inferred from the geometry of the Neogene Cerdanya basin (Fig. 24). It has been shown by GOURINARD (1971) that this basin is an asymmetric structure bordered by major E–W and NE–SW striking faults on its southern and eastern sides. The thickness of the basinfill sediments rapidly decreases towards the north, where only minor adjustment structures have been detected. The Cerdanya basin can therefore be considered to be an asymmetrical pull-apart type structure (CROWELL 1974), generated by a sinistral compo-

nent of horizontal movement on the Alt Segre fault. As rocks of Miocene and Pliocene age have been deposited in the basin, the fault must have been active during that timespan. The occurrence of a very large earthquake (epicentral intensity XI) in the Cerdanya Basin on 2-2-1428 (FOURNIGUET et al. 1981), shows that the faults are, geologically speaking, still active today.

There are a some indications that the Alt Segre fault extends westward into the Orri dome. Firstly, the abrupt termination of a major overturned Variscan mainphase fold-limb (Fig. 24) suggests the existence of an anomalous contact. Secondly, differences in style, size and orientation of folds do occur across the postulated continuation of the Alt Segre fault zone, such as the geometry of D_{V4} folds (isoclinal in the south, open to tight in the north). Further westward, the Alt Segre fault most likely joins up with the northern boundary fault of the Nogueras Zone, which explains the sudden change in strike of post-Variscan deposits that overlie the Orri dome unconformably (Fig. 24).

In conclusion, post-Alpine faulting is of divergent oblique-slip nature, involving a sinistral horizontal component of movement of unknown, but probably small magnitude. In spite of the frequent occurrence of normal dip-slip movement on east-west faults, including the large offset on the Alt Segre fault, the north-south extension related to normal faulting must have been limited because of the steep attitude of the fault planes.


Lineament analysis

A photogeological study of the Orri dome and surroundings reveals the presence of numerous well-defined lineaments. Without exception, they run perfectly straight across terrane with strong vertical relief so that it may be assumed that the lineaments represent subvertical planes. In some areas of good outcrop and monotonous lithology (e.g. in Permian redbeds), lineament traces can be easily correlated with (cemented) fractures in the field. The occurrence of lineaments is therefore attributed to brittle deformation affecting the rocks. Consequently, a directional analysis of lineament directions may throw light on the possible relations between fractures seen on aerial photographs and structures observed in outcrop.
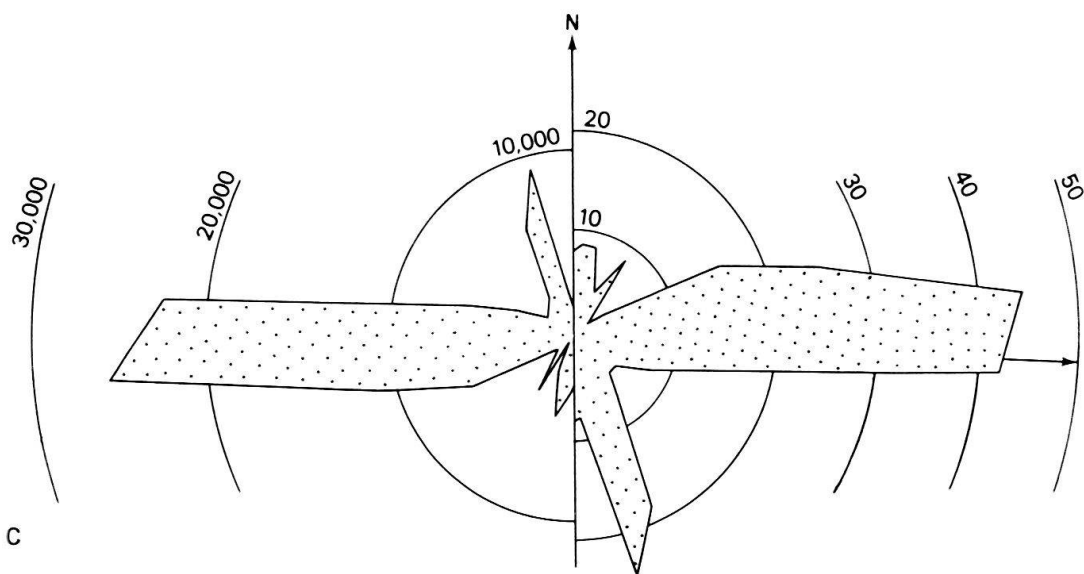

Fig. 25. Lineament analysis in the Orri dome.

a) Outline of the Orri dome, indicated by the outcrop area of Cambro-Ordovician rocks, and location of two subareas (of a total 69) referred to in Figs. 25 b and c. The area covered by Figure 26 is also shown.

b) Lineaments obvserved in the western part of the dome (Fig. 25 a). The left-hand part of the diagram shows length distribution of the lineaments per 10° interval (scale in meters), the right-hand part shows their frequency distribution. The distributions have a non-uniform character and the abundance of E–W lineaments suggests a unimodal nature of the distributions. Hence it is justified to apply a Rayleigh significance test for unimodality to our data. Transformation of the data set to double directional angles allows us to determine the (double) resultant vector directions for each distribution; in the present case the calculated orientation of the resultant vector is $\Theta = 90.1°$. The magnitude of the normalised resultant vector amounts to $\alpha = 0.428$. The Rayleigh test suggests a unimodal character of the distribution at 99 % confidence level (in spite of the occurrence of a relatively minor but persistent NNW–SSE component). Total number of lineaments $N = 276$, accumulated lineament length $\Sigma L = 144,150$ m.

c) Lineaments from a subarea in the southern Orri dome (Fig. 25 a). Length distribution is shown on the left (scale in meters) and frequency distribution to the right. The direction of the resultant vector: $\Theta = 93.2°$, its normalised magnitude $\alpha = 0.278$ (unimodal at 99 % confidence level). Total number of measurements $N = 254$, accumulated length $\Sigma L = 114,222$ m.
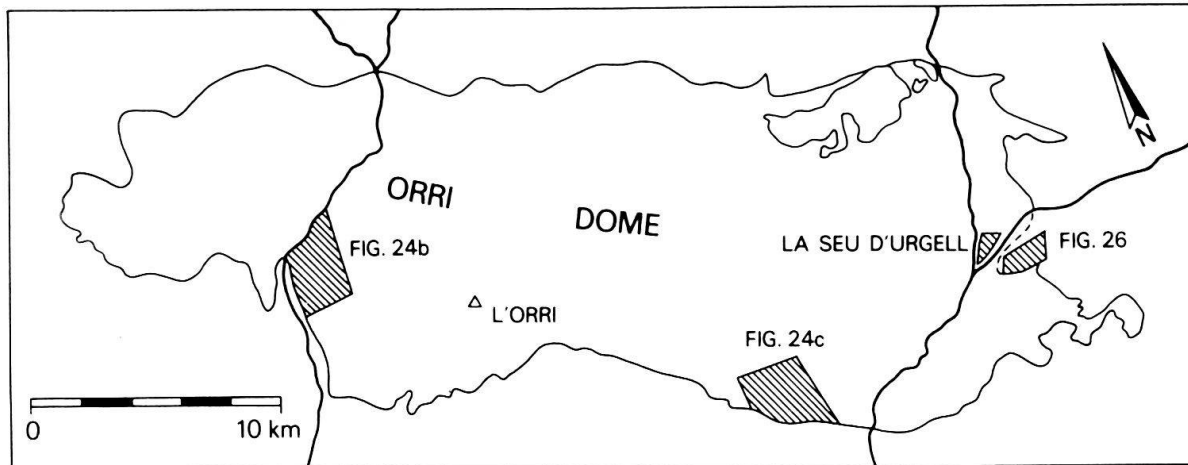
a
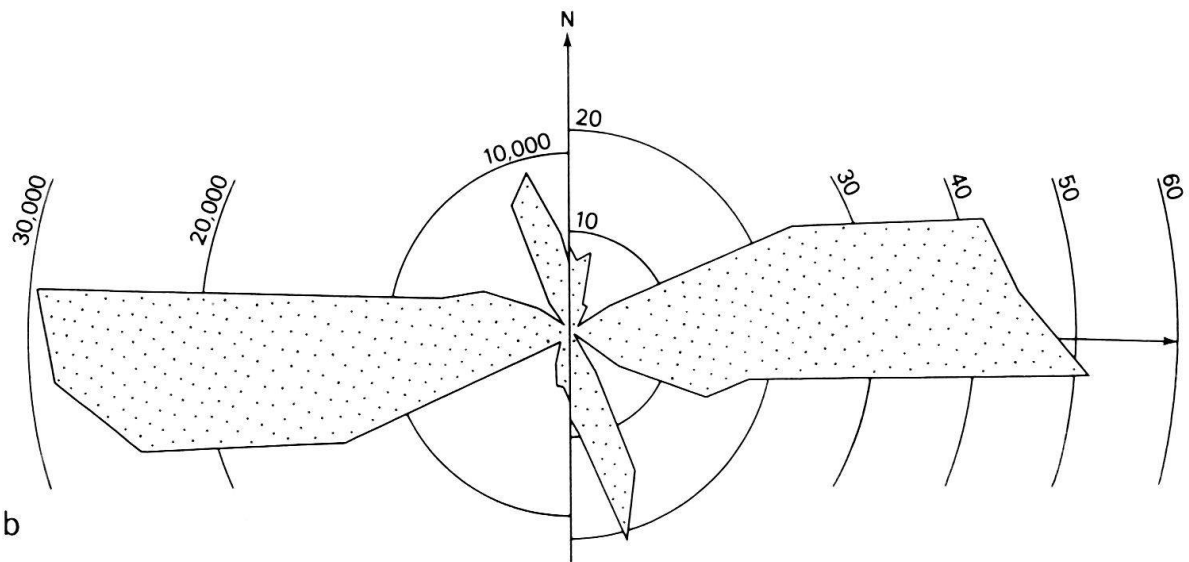
b

c

For this purpose, the exposure area of Cambro-Ordovician rocks in the Orri dome has been subdivided into 69 subareas (cf. Fig. 25 a), in which length and orientation of each lineament were determined. In total some 11 000 lineaments were measured, representing a total length of over 6500 km. In all subareas, E–W lineaments are abundant, while NNW–SSE directions occur frequently (Fig. 25 b and c). A simple Rayleigh significance test for the calculated resultant vector magnitudes of the distributions suggests unimodality in each subarea at 99 % confidence level, in spite of the occurrence of a small but persistent NNW–SSE trend. Furthermore, the directions of resultant vectors per subarea turn out to be very constant over the dome, as they only vary between 87.7°–267.7° and 95.3°–275.3°. (For an outline of calculation methods and significance tests see the caption to Figure 25 and CURRAY 1956).
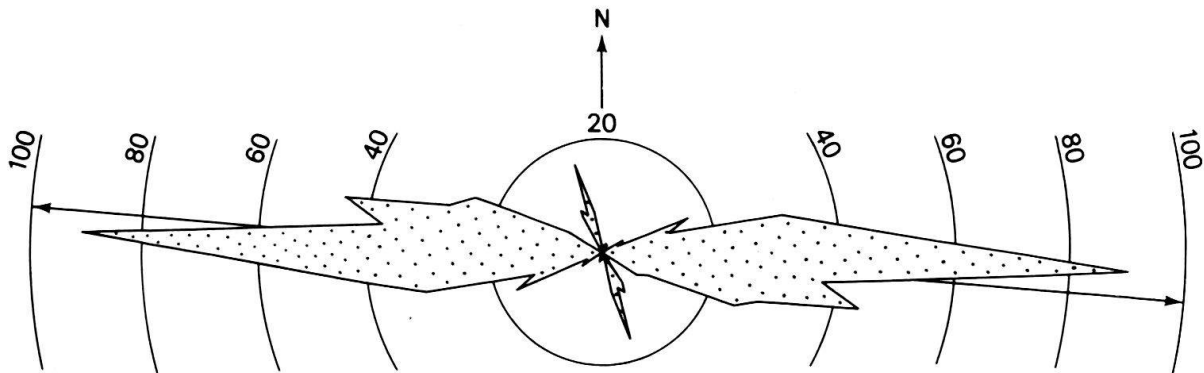

Fig. 26. Frequency distribution of lineaments in Pliocene rocks just east of the Orri dome (see Fig. 25 a). Total number of readings N = 460, direction of resultant vector (indicated by the arrow): Θ = 95.1°, magnitude of normalised resultant vector α = 0.716 (unimodal at 99 % confidence level).

Similar (but less detailed) results were obtained from photogeological studies of areas surrounding the Orri dome in which younger rocks are exposed. Figure 26 shows, as an example, the lineament direction distribution within unconsolidated Pliocene rocks just east of the dome. East-west lineaments are also frequently developed in the Quarternary alluvial deposits around La Seu d'Urgell (Fig. 2).

We may conclude that lineament (fracture) directions are more or less constant over the entire investigated area, irrespective of the age of the rocks in which they have developed.

The steep fractures observed in the field are some mm to some cm in width, and are either extensional fractures and/or dilatational shear fractures. Their nature therefore suggests that they may be of post-Variscan or post-Alpine age, also because they transect Variscan structures. The fact that the fractures have not only been observed in Paleozoic to Tertiary rocks but even in recent alluvial sediments, would rather indicate that they all developed, geologically speaking, extremely recently.

It seems more realistic to assume that fracturing in the Orri dome has been a more or less continuous process, involving generation of new fractures and reactivation of existing fractures whenever conditions were favourable to this effect (in terms of magnitude and direction of stress fields, material properties, strain rates, etc.). Extensional fractures and dilatational shear fractures now observed in the field and on aerial photographs may thus have been generated and/or reactivated at any moment in essentially extensional

structural regimes which existed during Paleozoic basin development (SPEKSNIJDER 1987), in the post-Variscan stage, or in the post-Alpine stage up to recent times (with the restriction that reactivated pre-Alpine fractures should not have been significantly over-printed by Variscan or Alpine deformation).

The present-day in-situ maximum principal stress σ_1 is vertical at the free surface, and σ_2 and σ_3, the intermediate and minimum stress components, lie within the horizontal plane. The vertical E–W open fractures, abundantly exposed today, have probably opened at right angels to σ_3, which would therefore be oriented N–S. This is in accordance with the overall extension in that direction during earlier post-Alpine deformation. Fractures with orientations other than E–W (see Fig. 25 and 26), appear to be (dilatational) shear fractures, reactivated in the present-day stress-field as they were oriented "favourably" with respect to the principal stresses σ_2 and σ_3 to allow for (renewed?) shearing (SIBSON 1985). The fact that some lineament orientations are completely lacking in the Orri dome (e.g. NE–SW and NW–SE) does not necessarily mean that fractures with these orientation do not occur, but rather that, if they were present, their orientations prevented them from being reactivated in the recent regional stress field. Hence, they do not show up as lineaments on aerial photographs.

Summary

As this study is constrained by the dimensions of the Orri dome and the age of the investigated rocks, no comprehensive correlation exercise of our data with other areas has been undertaken. As far as Variscan deformation is concerned, correlation within the Axial Zone turns out to be difficult anyway (ZWART 1981). For regional overviews regarding the structure of the Pyrenees the reader may consult ZWART (1979), MULLER & ROGER (1977), ARTHAUD & MATTE (1977), SOUQUET et al. (1977), SEGURET (1970), WILLIAMS (1985), SPEKSNIJDER (1987), and many others.

In the area of the present-day Orri dome, minor basin development occurred during the Early Paleozoic. There are no indications for major Caledonian deformation. Strong subsidence and basin differentiation took place in the Devonian and Early Carboniferous in a divergent oblique-slip setting (SPEKSNIJDER 1987). When conditions changed from divergent to convergent wrenching, early N–S folds were generated (D_{V1}). Progressive convergence subsequently resulted in the development of open E–W folds (D_{V2}), tight ESE–WNW mainphase folds (D_{V3}) characterised by a penetrative foliation, and D_{V4} folds which are coaxial to mainphase folds, but of smaller dimensions.

The latest stage of the Variscan orogeny is characterised by minor folds (D_{V5}) and compressional kinkbands (D_{V6}) which might be of only local significance. In the post-Variscan stage important lateral movements took place (D_{PV1}), accompanied by extensional features referred to as D_{PV2} (cleavage fanning) and D_{PV3} (kinkbands). One of the main results of this study is that the occurrence of relatively deep-seated D_{PV1} shearing can be directly correlated with superficial faulting and sedimentation in the Upper Carboniferous–Permian (SPEKSNIJDER 1985).

No record of Mesozoic deformation has been preserved in the Orri dome or its direct vicinity.

Important compression took place in the Eocene and Oligocene (Pyrenean phase of Alpine deformation). As a result, large nappes, including Paleozoic rocks of the Orri

dome, were emplaced towards the southern foreland. The last stage of deformation in the southern Pyrenees has been extensional, resulting in the generation and/or reactivation of minor fractures, as well as large-scale fault systems which transect all older structures.

The shape of the Orri dome as it outcrops today results mainly from interference between Variscan pre-mainphase (D_{V1} and D_{V2}), mainphase (D_{V3}), and first refolding (D_{V4}) structures, modified by post-Variscan faulting and shearing, Alpine thrusting and post-Alpine faulting.

Acknowledgments

REFERENCES

ARTHAUD, F. & MATTE, P. (1977): Late Paleozoic strike-slip faulting in southern Europe and northern Africa: Result of right-lateral shear zone between the Appalachians and the Urals. – Bull. Geol. Soc. Amer. *88*, 1305–1320.

BOSCHMA, D. (1963): Successive Hercynian structures in some areas of the Central Pyrenees. – Leidse Geol. Meded. *41*, 153–220.

BROUWER, TH. N. (1968): Verslag van een geologische kartering in de omgeving van de Cerdaña vallei, oostelijke Pyreneeën, Spanje. – Internal rep. Leiden University.

CROWELL, J.C. (1974): Sedimentation along the San Andreas Fault, California. In: R.H. DOTT, Jr. & R.H. SHAVER (Ed.): Modern and ancient Geosynclinal Sedimentation. – Spec. Publ. Soc. Econ. Paleont. Miner. *19*, 292–303.

CURRAY, J.R. (1956): The analysis of two-dimensional orientation data. J. Geol. *64*, 117–131.

DONATH, F.A. (1969): Experimental study of kink-band development in strongly anisotropic rock. In: A.J. BAER & D.K. NORRIS (Ed.): Proc. Conf. on research in tectonics (Kinkbands and brittle deformation), Ottawa, March 1968 – Geol. Surv. Canada, Pap. 68–52, 255–287.

FOURNIGUET, J., VOGT, J. & WEBER, C. (1981): Seismicity and recent crustal movements in France. – Tectonophysics *71*, 195–216.

GOURINARD, Y. (1971): Détermination cartographique et géophysique de la position des failles bordières du fosse néogene de Cerdagne (Pyrénées orientales franco-espagnoles). – 96ᵉ Congr. nat. Soc. Sav. Toulouse, II, 245–263.

HARTEVELT, J.J.A. (1970): Geology of the Upper Segre and Valira valleys, Central Pyrenees, Andorra/Spain. – Leidse Geol. Meded. *45*, 167–236.

HOBBS, B.E., MEANS, W.D. & WILLIAMS, P.F. (1976): An outline of structural geology. – John Wiley & Sons, Inc., New York.

HOEPPENER, R. (1955): Tektonik im Schiefergebirge. – Geol. Rdsch. *44*, 26–58.

LAMOUROUX, C., SOULA, J.-C. & RODDAZ, B. (1981): Les zones mylonitiques des massifs du Bessiès et de l'Aston (Haute Ariège). – Bull. B.R.G.M., I, 2, 103–111.

MEY, P.H.W. (1967 b): The geology of the Upper Ribagorzana and Baliera valleys, Central Pyrenees, Spain. Leidse Geol. Meded. *41*, 153–220.

— (1968): Geology of the Upper Ribagorzana and Tor valleys, Central Pyrenees, Spain. – Leidse Geol. Meded. *41*, 229–292.

MEY, P.H.W., NAGTEGAAL, P.J.C., ROBERTI, K.J. & HARTEVELT, J.J.A. (1968): Lithostratigraphic subdivision of post-Hercynian deposits in the South-Central Pyrenees, Spain. – Leidse Geol. Meded. *41*, 221–228.

MULLER, J. & ROGER, PH. (1977): L'évolution structurale des Pyrénées (domaine central et occidental). Le segment hercynien, la chaîne de fond alpine. – Géol. Alp. *3*, 149–191.

MUÑOZ, J.A., MARTINEZ, A. & VERGES, J. (1986): Thrust sequences in the eastern Spanish Pyrenees. – J. Struct. Geol. *8*, 399–405.

NAGTEGAAL, P.J.C. (1969): Sedimentology, paleoclimatology, and diagenesis of post-Hercynian continental deposits in the south-central Pyrenees, Spain. – Leidse Geol. Meded. *42*, 143–238.

PARISH, M. (1984): A structural interpretation of a section of the Gavarnie nappe and its implications for Pyrenean geology. – J. Struct. Geol. *6*, 247–255.

PATERSON, M.S. & WEISS, L.E. (1966): Experimental deformation and folding in phyllite. – Bull. Geol. Soc. Amer. *77*, 343–374.

POWELL, C.McA., COLE, J.P. & CUDAHY, T.J. (1985): Megakinking in the Lachlan Fold Belt, Australia. – J. Struct. Geol. *7*, 281–300.

RAMSAY, J.G. (1962b): The geometry of conjugate fold systems. – Geol. Mag. *99*, 516–526.

— (1967): Folding and fracturing of rocks. – McGraw-Hill, New York.

SCHMIDT, H. (1931): Das Paläozoikum der spanischen Pyrenäen. – Abh. Ges. Wiss. Göttingen math.-phys. Kl. 3, Folge H. 5, 8, 1–85.

SEGURET, M. (1970): Etude tectonique des nappes et séries décollées de la partie centrale du versant sud des Pyrénées. – Ph. D. thesis, Montpellier.

SIBSON, R.H. (1985): A note on fault reactivation. – J. Struct. Geol. *7*, 751–754.

SITTER, L.U. DE (1965): Hercynian and Alpine orogenies in northern Spain. Geol. Mijnbouw *44*, 373–383.

SOLE SUGRAÑES, L. (1978): Alineaciones y fracturas en el sistema Catalan a segun las imagenes Landsat-1. – Tecniterrae *22*, 1–11.

SOUQUET, P., PEYBERNES, B., BILOTTE, M. & DEBROAS, E.-J. (1977): La chaîne alpine des Pyrénées. – Géol. Alp. *53*, 193–216.

SPEKSNIJDER, A. (1985): Anatomy of a strike-slip fault controlled sedimentary basin, Permian of the southern Pyrenees, Spain. – Sediment. Geol. *29*, 31–66.

— (1987): The detection and significance of early deformation in the southern Variscan Pyrenees, Spain; implications for regional Paleozoic structural evolution. – Geol. Rdsch. *76*/2, 451–476.

WEISS, L.E. (1969): Flexural slip folding of foliated model materials. In: A.J. BAER & D.K. NORRIS (Ed.): Proc. Conf. on research in tectonics (Kink bands and brittle deformation); Ottawa, March 1968. – Geol. Surv. Canada, Pap. 68-52, 294–357.

WILLIAMS, G.D. (1985): Thrust tectonics in the south central Pyrenees. – J. Struct. Geol. *7*, 11–17.

WILLIAMS, G.D. & FISCHER, M.W. (1984): A balanced section across the Pyrenean orogenic belt. – Tectonics *3*, 773–780.

ZANDVLIET, J. (1960): The geology of the Upper Salat and Pallaresa valleys, Central Pyrenees, France/Spain. – Leidse Geol. Meded. *25*, 1–127.

ZWART, H.J. (1968): The paleozoic crystalline rocks of the Pyrenees in their structural setting – Krystalinikum *6*, 125–140.

— (1979): The geology of the central Pyrenees. – Leidse Geol. Meded. *50*, 1–74.

— (1981): Three profiles through the Central Pyrenees. – Geol. Mijnbouw *60*, 97–106.

ZWART, H.J. & ROBERTI, K.F. (1976): Geological map of the Central Pyrenees. Sheet 9: Flamisell-Pallaresa. – Geol. Inst. Leiden.